Universidade de Coimbra
Faculdade de Ciências e Tecnologia
Departamento de Ciências da Vida

Pathophysiology of persistent doxorubicin cardiotoxicity

Metabolic landscaping of the epigenome

Author:
André Ferreira

Supervisors:
Paulo J. Oliveira
António J. Moreno

June, 2015

André Ferreira: *Pathophysiology of persistent doxorubicin cardiotoxicity,* Metabolic landscaping of the epigenome, B.Sc. Biology, June 2015

This work was performed at the Center for Neuroscience and Cell Biology, Department of Life Sciences, University of Coimbra, Portugal, under the supervision of Dr. Paulo J. Oliveira (CNC, UC) and Dr. António J. Moreno (DCV, UC). Dr. Teresa Cunha-Oliveira also supervised the present work.

The work presented in this dissertation was funded by FEDER funds through the Operational Programme Competitiveness Factors – COMPETE and national funds by the Portuguese Foundation for Science and Technology (FCT) –, by an institutional grant UID/NEU/04539/2013 to the CNC and by QREN project "Stemcell based platforms for Regenerative and Therapeutic Medicine" [#4832, reference CENTRO-07-ST24-FEDER-002008] funded through FEDER/QREN 2007–2013. Also supported by a PhD fellowship from FCT to Filipa S. Carvalho (SFRH/BD/64694/2009) and by research grants to Dr. Paulo J. Oliveira (PTDC/DTP-FTO/1180/2012) and Dr. António Moreno (PTDC/SAU-OSM/104731/2008).

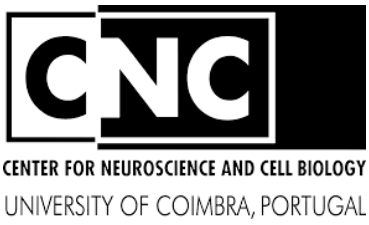

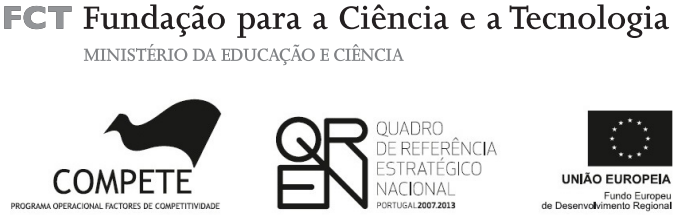

Acknowledgements

Firstly I would like to thank my supervisor Dr. Paulo Oliveira for introducing me to this project and without whose help this work could not have been possible. I would also like to thank Dr. Teresa Oliveira for her continuous advice, guidance, and most of all for her endless patience and time spent training me in most of what I currently know.

I would like to acknowledge the help and time given by all the people in the MitoXT group – past and present. The making of this thesis would have been a diabolical endeavor had it not been for the moments, minutes or hours of assistance given whenever the need for help arose. Many thanks in particular for the multiple times when someone volunteered to finish my experiments or take care of my mess every time I was running late for my ride back home.

Abstract

Doxorubicin (DOX), a potent and broad-spectrum antineoplastic agent, causes a cumulative dose-dependent cardiomyopathy of late-onset that may ultimately lead to congestive heart failure. The mechanisms responsible for the delayed nature of DOX cardiotoxicity remain poorly understood. Since DOX induces a persistent depression in cardiomyocyte gene expression patterns, it is reasonable to hypothesize that a "toxicity memory" is being formed by means of epigenetic modulation. To test this hypothesis, eight week-old male Wistar rats ($n = 6$ per group) were administered 7 weekly injections with DOX ($2\,\mathrm{mg\,kg^{-1}}$) or equivalent volume of saline solution and sacrificed two weeks after the last injection. We assessed gene expression patterns by qPCR, global DNA methylation by ELISA and proteome lysine acetylation status by Western blot in cardiac tissue from saline and DOX-treated rats. We show for the first time that DOX treatment decreases global DNA methylation in a cardiac-specific fashion. These differences were accompanied by alterations in mRNA expression of multiple functional gene groups. Doxorubicin disrupted cardiac mitochondrial biogenesis, as demonstrated by reduced mtDNA levels and altered transcript levels for multiple mitochondrial genes encoded by both nuclear and mitochondrial genomes. Transcription of genes involved in lipid metabolism and epigenetic modulation were also disturbed. Western blotting analyses indicated a differential protein acetylation pattern in cardiac mitochondrial fractions of DOX-treated rats. Additionally, DOX treatment increased the activity of histone deacetylases. Overall, the results presented in this thesis support previous observations showing that DOX impairs cardiac mitochondrial function and induces a switch in substrate metabolism. These results are also consistent with the interplay between mitochondrial dysfunction and epigenetic alterations in the persistent nature of DOX-induced cardiotoxicity. One possibility is that DOX may modulate gene expression patterns via alterations to the epigenetic landscape, which could be related to a disturbance in metabolite availability.

Keywords: doxorubicin; epigenetics; heart; mitochondria; toxicology.

Resumo

A doxorubicina (DOX), um potente fármaco antineoplástico com um amplo espectro de acção, causa uma cardiomiopatia cumulativa, dose-dependente que em última instância pode levar a insuficiência cardíaca. Os mecanismos responsáveis por esta condição ainda não são conhecidos. Como a DOX induz uma depressão persistente nos padrões de expressão genética em cardiomiócitos, podemos teorizar que a DOX imprime uma "memória tóxica" por meio de modulação epigenética. Para testar esta hipótese, ratos machos Wistar Han com oito semanas de idade ($n = 6$ por grupo) receberam oito injecções subcutâneas semanais de DOX ($2\,\mathrm{mg\,kg^{-1}}$) ou de um volume equivalente de solução salina, sendo sacrificados duas semanas após a última injecção. O nosso trabalho identificou padrões de expressão genética por qPCR, metilação global de DNA por ELISA e o padrão de acetilação de lisinas no proteoma por Western blot em tecido cardíaco. Mostramos pela primeira vez que a DOX diminui os níveis de metilação global de DNA no tecido cardíaco. Este efeito foi acompanhado por alterações na expressão de mRNAs de vários conjuntos funcionais de genes. A DOX alterou a biogénese mitocondrial cardíaca, como identificado por uma redução dos níveis de mtDNA e alterações dos níveis de transcriptos de múltiplos genes mitocondriais codificados por ambos os genomas (nuclear e mitocondrial). A transcrição de genes envolvidos no metabolismo de lípidos e em modulação epigenética também foi alterada. Análises por Western blot revelaram um padrão de acetilação proteica diferente em fracções mitocondriais de animais tratados com DOX. Adicionalmente, o tratamento com DOX aumentou a actividade enzimática de deacetilases de histonas. Colectivamente, os resultados apresentados nesta tese suportam observações anteriores que mostram que a DOX perturba a função mitocondrial e induz uma substituição no substrato metabólico preferencial no coração, sendo também consistentes com a nossa hipótese de que uma acção recíproca entre disfunção mitocondrial e alterações epigenéticas é um factor importante na natureza persistente da toxicidade induzida pela DOX. Uma possível explicação é a de que a DOX modula os padrões de expressão genética através de alterações na paisagem epigenética, o que pode ser consequência de uma perturbação na disponibilidade de metabolitos.

Palavras chave: coração; doxorubicina; epigenética; mitocôndria; toxicologia.

Table of Contents

List of Figures

List of Tables

List of Acronyms and Abbreviations

5-MTHF	5-Methyl-tetrahydrofolate
Ac-CoA	Acetyl coenzyme A
ACL	ATP citrate lyase
CAT	Carnitine acetyltransferase
CACT	Carnitine–acylcarnitine translocase
cDNA	Complementary DNA
CPT1B	Carnitine palmitoyltransferase I B
Cyt *c*	Cytochrome *c*
DNMT	DNA methyltransferase
DOX	Doxorubicin
DTT	Dithiothreitol
ELISA	Enzyme-linked immunosorbent assay
ETC	Electron transport chain
FFA	Free fatty acid
GSH	Glutathione, reduced
HAT	Histone acetyl transferase
Hcy	Homocysteine
HDAC	Histone deacetylase
m^5C	5-Methylcytosine
MAT	Methionine adenosyltransferase
mtDNA	Mitochondrial DNA
nDNA	Nuclear DNA
NRF	Nuclear respiratory factor
OxPhos	Oxidative phosphorylation

PGC	Peroxisome proliferator-activated receptor gamma coactivator
PPAR	Peroxisome proliferator-activated receptor
qPCR	Quantitative real-time polymerase chain reaction
ROS	Reactive oxygen species
SAH	*S*-Adenosyl-L-homocysteine
SAL	Saline
SAM	*S*-Adenosyl-L-methionine
STM	Sucrose-Tris-magnesium
TBS-T	Tris-buffered saline with Tween
TFAM	Mitochondrial transcription factor A
THF	Tetrahydrofolate

Chapter 1

Introduction

1.1 Doxorubicin

Doxorubicin (Adriamycin®, DOX) was one of the first anthracyclines* to be isolated from strains of *Streptomyces* actinobacteria in the 1960s (Arcamone et al., 1969). Since its clinical introduction in the 1970s, DOX has remained one of the most important components in several currently used chemotherapy protocols for treating breast, ovarian and gastric carcinomas, sarcomas, leukemias, non-Hodgkin's and Hodgkin's lymphoma, multiple myeloma and many other cancers (Sterba et al., 2013; Simunek et al., 2009). The impact of anthracycline-based therapies in the field of oncology is particularly noteworthy in pediatric oncology, where the 5-year survival rate for childhood cancer has increased from around 30 % in the 1960s to over 70 % in the modern era, which explains why over 50 % of childhood cancer survivors are estimated to have received anthracycline treatment (Sterba et al., 2013; Simunek et al., 2009).

Figure 1.1 shows the chemical structure of DOX. It contains the basic structure of all anthracyclines, which is a tetracyclic anthraquinone-containing aglycone linked to an aminosugar, and is distinguished mainly by a short side chain with a carbonyl group at C-13, a hydroxyl group at C-14 and the aminosugar daunosamine attached by a glycosidic bond to the C-7 of the tetracyclic ring. Because the anthracycline template has so much potential for modification, more than 2000 structural variants of this class of compounds have been produced and tested for antitumor activity in an effort to find more effective and safer chemotherapeutic agents (Krohn, 2008). None of them have shown any significant advantage over previously existing compounds, and thus only a small number of anthracyclines are currently employed in clinical settings – DOX and Daunorubicin, the first anthracyclines to be isolated, being among the most relevant ones (Krohn, 2008).

Despite having over 40 years of extensive clinical utilization, DOX's mechanism of action remains a matter of controversy to this day, as novel mechanisms are continuously being proposed. The cytostatic and cytotoxic actions of DOX in cancer cells have been attributed to various mechanisms, most often: 1) DNA

*Anthracyclines are defined as red–orange dyes containing a skeleton of 7,8,9,10-tetrahydrotetracene-5,12-quinone with mono- to tetrasaccharide moieties attached, usually to ring D of the aglycone (Laatsch and Fotso, 2008).

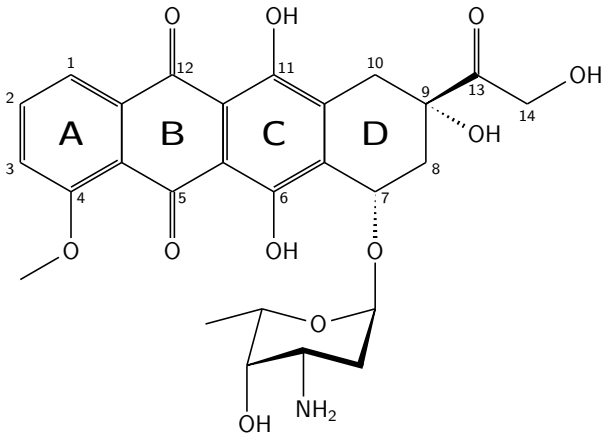

Figure 1.1. Chemical structure of Doxorubicin.

intercalation, 2) topoisomerase II inhibition, 3) generation of free radicals with consequent induction of oxidative stress and 4) apoptosis induction – although probably as an outcome of the aforementioned events (Gewirtz, 1999). Novel alternative mechanisms recently proposed include inhibition of DNA methylation enzymes (Yokochi and Robertson, 2004) and nucleosome destabilization induced by chromatin torsional stress (Yang et al., 2014). This diversity of antitumor mechanisms is likely to underlie the broad spectrum of activity displayed by DOX.

As is the case for every anticancer agent, DOX is a double-edged sword due to its toxic side effects in healthy tissue – cardiac muscle tissue in particular. Administration of DOX commonly results in relatively harmless short-term acute effects such as nausea, diarrhea, alopecia and electrocardiography alterations that are frequently reversible (Sterba et al., 2013; Carvalho et al., 2009). Chronic cardiotoxic effects, on the other hand, are of much greater concern. Cumulative doses exceeding 500–550 mg/m^2 result in a clinically unacceptable risk of developing congestive heart failure (CHF) (Lefrak et al., 1973), thus severely limiting the clinical utility of this compound. The onset of this cardiomyopathy may be delayed until as many as 20 years after cessation of treatment (Steinherz et al., 1991).

The mechanisms by which this cardiotoxicity arises appear to be very different from the ones responsible for DOX's antitumor activity. A plausible consequence of this observation is the possibility of developing cardioprotective treatment protocols that can be performed in parallel with DOX-based chemotherapeutic protocols withouth diminishing the drug's efficacy.

1.1.1 Antitumor activity

As previously mentioned, DOX's antitumor activity is mostly atributted to various DNA-related interactions, as would be expected given the reliance of rapidly proliferating tumor cells on DNA integrity.

DNA intercalation

Some of the earliest studies addressing the antitumor activity of anthracyclines reported an inhibition of both DNA and RNA synthesis (Di Marco et al., 1965;

Bremerskov and Linnemann, 1969) and a high affinity of anthracyclines for DNA (Calendi et al., 1965). Naturally, DNA binding was promptly suggested as the mechanism underlying the antitumor activity of anthracyclines. Indeed, DNA-anthracycline interactions have been confirmed by numerous sources of evidence over time, from X-ray diffraction studies (Quigley et al., 1980; Nunn et al., 1991) to in silico analyses (Box, 2007).

The chemical structure of anthracyclines makes them suitable DNA intercalating agents. Under the double helical structure, DNA can accommodate the planar tetracyclic ring between neighboring base pairs. This DNA-anthracycline complex is further stabilized by electrostatic interactions between the negatively charged DNA phosphate backbone and the positively charged amino group of the aminosugar (Box, 2007; Beretta and Zunino, 2008). DNA intercalation is known to occur at clinically relevant concentrations of DOX (Coldwell et al., 2008), however only a very small fraction of total DOX participates in this process (Yang et al., 2014). DNA intercalation is therefore unlikely to be the most significant mediator of DOX's antitumor activity.

Topoisomerase II poisoning

DNA topoisomerases are enzymes responsible for removal of knots and tangles generated during nuclear processes such as DNA replication and transcription. Topoisomerase II in particular is of critical importance, since its activity is absolutely required for chromosome segregation and therefore cell cycle progression (Nitiss, 1998). One step in the catalytic cycle of this enzyme consists in the introduction of a short-lived double-strand DNA break that allows for the relaxation of supercoils, thereby restoring functional DNA topology (Champoux, 2001). A covalent enzyme-DNA complex – referred to as the "cleavable complex" – is established during this step, so as to safely sequester, process and repair the topoisomerase II-mediated double-stranded DNA breaks (Wilstermann and Osheroof, 2003). Many anthracyclines (DOX included) belong to the class of drugs known as topoisomerase II poisons, which stabilize the cleavable complex and prevent the DNA religation step (Larsen et al., 2003). Increasing the lifetime of this complex enhances the likelihood of incorrectly resolving the DNA breaks via, for example, illegitimate recombination events. Moreover, if left unresolved, DNA breaks will trigger the DNA damage response and ultimately lead to apoptosis.

Oxidative stress

Generation of free radicals by DOX can occur through multiple pathways. Doxorubicin is a suitable substrate for many flavoenzymes that catalyze the oxidation of NAD(P)H, such as the cytosolic eNOS (Vasquez-Vivar et al., 1997), the endoplasmic reticulum and nuclear envelope cytochrome P450 reductase (Bachur et al., 1977; Bachur et al., 1982) and the mitochondrial NADH dehydrogenase (complex I) (Davies and Doroshow, 1986). The one-electron reduction of DOX initiates a futile redox cycle (depicted in Fig. 1.2) that generates superoxide anions ($O_2^{\bullet -}$). Superoxide can then inactivate Fe–S cluster-containing enzymes (Flint et al., 1993), releasing in the process ferrous iron (Fe^{2+}) that will in turn assist in

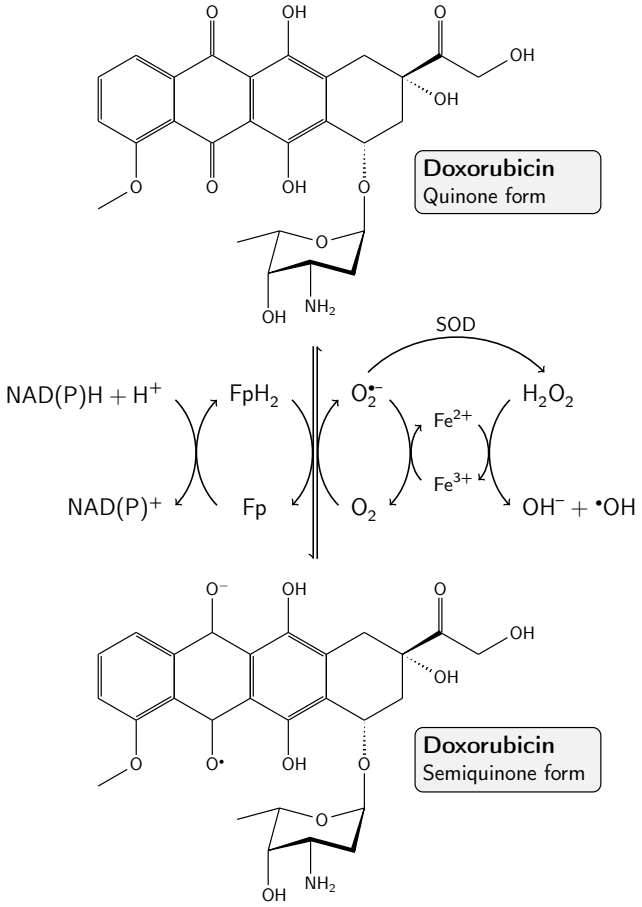

Figure 1.2. Formation of ROS through DOX redox cycling. The quinone form of DOX accepts an electron from either NADH or NADPH, in a reaction catalized by flavoprotein-containing enzymes such as NADH dehydrogenase (complex I) or cytochrome P450 reductase. The resulting semiquinone radical cycles back to its quinone form upon transfering an electron to O_2, thereby generating $O_2^{\bullet -}$. Additional ROS can be formed in subsequent reactions, including the highly reactive $^{\bullet}OH$.

the iron-catalyzed Haber–Weiss reaction, leading to the formation of the highly reactive hydroxyl radical ($^{\bullet}OH$) (Halliwell and Cross, 1994). Another suggested mechanism is the formation of DOX-Fe complexes, in which the cycling between Fe^{2+} and Fe^{3+} begets superoxide and hydroxyl radicals (Simunek et al., 2009). Cancer cells appear to demonstrate increased steady-state levels of oxidative stress when compared to normal cells (Aykin-Burns et al., 2009), and therefore are likely to be more susceptible to apoptosis induction via increased reactive oxygen species (ROS) generation.

1.1.2 Cardiotoxicity

A variety of mechanisms have been proposed to be responsible for the development of DOX-induced cardiotoxicity. Mitochondrial interactions are some of the most implicated and best described mechanisms, and will be explored in greater detail

below.

Mitochondria-dependent toxicity

Cardiac muscle possesses one of the highest mitochondrial density values (ca. 30 % cellular volume) of all tissues in the organism (Barth et al., 1992), reflecting its reliance on mitochondrial metabolism for energy production. Indeed, cardiomyocytes obtain over 90 % of their ATP through oxidative phosphorylation (OxPhos) (Ventura-Clapier et al., 2004). As such, the heart is a vulnerable organ to drugs that target mitochondria, as is the case of DOX. Mitochondrial ultrastructural alterations were in fact one of the earliest features to be identified in DOX cardiotoxicity (Friedman et al., 1978; Aversano and Boor, 1983).

Doxorubicin has been shown to preferentially accumulate in cardiac tissue (Peters et al., 1981). The driving force behind this uptake is likely related to the elevated mitochondrial content displayed by this tissue. Doxorubicin binds with high affinity to cardiolipin (Goormaghtigh et al., 1980), a unique phospholipid found almost exclusively in the inner mitochondrial membrane, and is retained in mitochondria as a result (Nicolay et al., 1986). Consequently, DOX is brought to close proximity of the electron transport chain (ETC), facilitating the occurrence of the aforementioned redox cycling in complex I. Moreover, cardiolipin-protein interactions are essential for proper assembly and function of ETC proteins. Formation of DOX-cardiolipin complexes disrupts these interactions, possibly leading to increased rates of electron leak (and thus, ROS formation) from the ETC (Schlame et al., 2000).

If mitochondria are a major site of DOX-induced ROS formation, it follows that mitochondria should also be a prime target for oxidative stress. This should be especially the case for cardiac mitochondria, as cardiac tissue displays relatively low levels of antioxidant defenses when compared to other organs including the liver (Doroshow et al., 1980). Consistent with this idea are the findings that DOX treatment results in several oxidative stress markers in cardiac mitochondria, such as lipid peroxidation (Mimnaugh et al., 1985), protein carbonylation (Ascensao et al., 2006; Suliman et al., 2007) and mitochondrial DNA (mtDNA) oxidation (Palmeira et al., 1997; Serrano et al., 1999). Studies using transgenic animal models overexpressing mitochondrial exclusive (MnSOD) and non-exclusive (Gpx1) antioxidant enzymes have shown beneficial effects in DOX-induced cardiotoxicity (Yen et al., 1999; Xiong et al., 2006), further reinforcing the role of oxidative stress as a major culprit.

Not surprisingly, many of the expected functional consequences of mitochondrial dysfunction have been reported for this pathology. Lipid peroxidation – particularly of the acyl chains in cardiolipin – not only compromises ETC function, as already mentioned, but also contributes to apoptosis. Cytochrome *c* (Cyt *c*), one of the ETC proteins that exists in close association with cardiolipin, has a pivotal role in the intrinsic pathway of apoptosis, where its translocation from the intermembrane space to the cytosol is one of the required events (Raha and Robinson, 2001). It has previously been shown that Cyt *c* translocation is a two-step process, requiring both the permeabilization of the outer mitochondrial membrane and the detachment of Cyt *c* from the inner membrane (Ott et al., 2002). This

last step occurs as a result of cardiolipin peroxidation, which compromises its ability to interact with Cyt *c*. Loss of mitochondrial calcium homeostasis and the concurrent activation of the mitochondrial permeability transition are also likely to contribute to apoptotic signaling (Solem et al., 1994; Zhou et al., 2001a). Both the release of Cyt *c* and the ensuing activation of apoptosis have been confirmed in cardiomyocytes of DOX-treated rats (Childs et al., 2002). Finally, impairment of overall OxPhos metabolism has also been extensively documented in murine models, as shown by the inhibition of ETC protein activity (Santos et al., 2002; Chandran et al., 2009), decreased state 3 respiration (oxygen consumption associated with ATP synthesis) (Solem et al., 1994; Santos et al., 2002), increased state 4 respiration (basal oxygen consumption) (Ji and Mitchell, 1994) and decreased ATP/ADP ratio (Oliveira et al., 2004).

Persistent cardiotoxicity

All the above notwithstanding, a satisfying explanation for the continued development of cardiotoxicity is yet to be found. It is clear from the progressive development of cardiomyopathy that DOX somehow imprints cardiomyocytes with what can be considered a "toxic memory". This notion is supported by one of the few studies that employed a delayed model of DOX toxicity in vivo. The authors reported a sustained increase in oxidative stress after a recovery time of 5 weeks – greater than the increase observed after 1 week of recovery (Zhou et al., 2001b) – suggesting that DOX imprinted a ROS-generating mechanism that is not directly mediated by the drug itself. One possible mechanism that has been suggested to be involved in this toxic memory is the oxidation of mtDNA (Berthiaume and Wallace, 2007a). Indeed, DOX was reported to induce a variety of persistent insults to mtDNA in both animal models (Lebrecht et al., 2003) and human patients (Lebrecht et al., 2005). However, based on a number of observations, we consider that the possibility of long-term epigenetic modulation is a hypothesis worthy of investigation. Results from global gene expression arrays reveal that gene expression patterns – the endpoint of epigenetic modulation – are altered in rats for up to 5 weeks after DOX treatment (Berthiaume and Wallace, 2007b). The study reported a curious trend in metabolic genes: genes involved in fatty acid oxidation were found to be downregulated while genes related to glycolysis were upregulated. The physiological implication of these findings was later substantiated by ^{13}C-isotopomer analyses (Carvalho et al., 2010), which confirmed the switch from the preferential oxidation of fatty acids to a more glycolytic metabolism. Collectively, these results suggest that DOX induces a long-term metabolic remodeling in cardiac tissue by acting at the transcriptional level, as opposed to the aforementioned short- to medium-term effects on OxPhos metabolism that are dependent on the presence of the drug. Both the observed alterations in the transcriptome and the previously alluded to "toxic memory" concept would be consistent with DOX-induced persistent alterations in the epigenetic landscape.

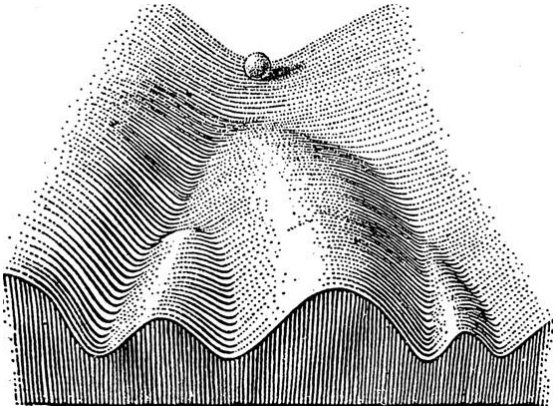

Figure 1.3. Conrad Waddington's visual metaphor for the epigenetic landscape. The immature cell depicted at the top of the landscape is offered a set of paths towards potential differentiation outcomes. Initial inputs determine which path will be followed, but a change in course is possible upon overcoming a certain threshold. Figure from Waddington (1957).

1.2 Epigenetics, and the bioenergetics thereof

The concept of epigenetics dates back to when DNA was yet to be identified as the molecule of inheritance. In 1942, Conrad Waddington defined epigenetics as "the branch of biology which studies the causal interactions between genes and their products, which bring the phenotype into being". This concept was Waddington's attempt at bridging the gap between genetic information and observable phenotypes that could not be accounted for by Mendelian inheritance. To this day, Waddington's depiction of what he called the "epigenetic landscape" (Fig. 1.3) remains an adequate analogy for the concept.

Modern definitions of epigenetics refer to post-translational and chemical modifications of chromatin that do not alter the genomic sequence itself (Berger et al., 2009).* Chromatin is composed of repeating units of nucleosomes, each consisting of a 147 bp DNA segment wound around a histone octamer composed of two copies of each of the four core histones proteins H2A, H2B, H3 and H4 (Luger and Hansen, 2005). Structurally, the core histones are mostly globular, with the exception of unstructured extensions protruding from the nucleosome core that are known as "histone tails". Chromatin post-translational modifications occur at the level of histones – particularly in the tail regions of histones H3 and H4 (Kouzarides, 2007; Bannister and Kouzarides, 2011). Post-translational modifications described thus far include acetylation, methylation, phosphorylation, ubiquitylation, sumoylation (SUMO: small ubiquitin-like modifier), ADP ribosylation, deimination and proline isomerization (Kouzarides, 2007). The majority of histone post-translational modifications are dynamic, and in normal conditions are regulated to adequately fit particular cellular contexts. Chemical modifications of chromatin, in turn, occur at the level of DNA, mainly in CpG dinucleotides. These include DNA methylation and hydroxymethylation (Guibert and Weber, 2013). Collectively, epigenetic modifications regulate the regional architecture of chromatin, thereby controlling the accessibility of DNA to proteins such as transcription factors and ultimately determining gene expression patterns. Epigenetic modifications, in turn, are regulated by at least three factors: the expression levels of chromatin-modifying enzymes, signaling pathways that recruit

*Many authors further consider noncoding RNA-mediated chromatin regulation (Collins et al., 2011; Rinn and Chang, 2012) and transvection (Pirrotta, 1999) – a phenomenon that refers to interchromosomal interactions between homologous alleles – as epigenetic mechanisms.

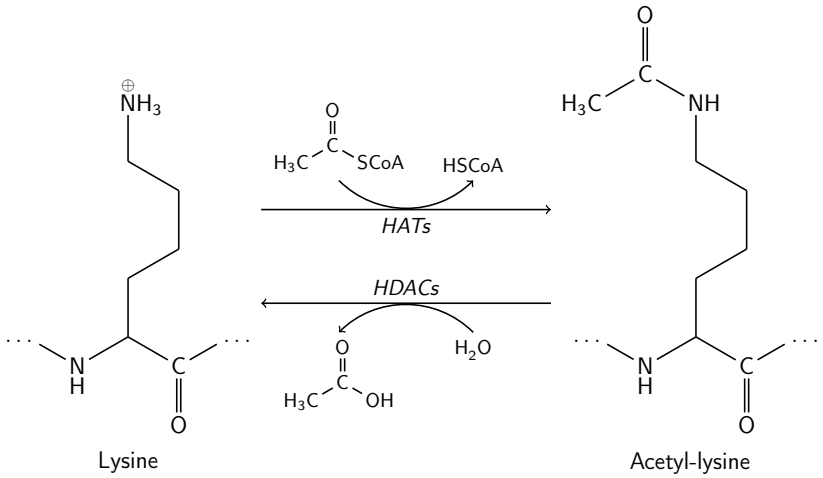

Figure 1.4. Acetylation and deacetylation cycle of histone lysine residues. Acetyl moieties are transfered from Ac-CoA to the ε-amino group of a lysine residue by HATs. The reverse reaction is performed by HDACs, which catalyze the hydrolysis of acetyl-lysine to yield lysine and acetate. Sirtuins can also catalyze the deacetylation of acetyl-lysine, although using a different catalytic mechanism from the one depicted here.

or displace these enzymes and the levels of substrates and cofactors required for their function (Lu and Thompson, 2012).

This section will limit the discussion to histone acetylation and DNA methylation, along with the metabolic requirements of both processes. Potential routes of interference by DOX will also be addressed.

1.2.1 Histone acetylation

Histone proteins have a positively charged surface owing to the abundant presence of basic amino acids (lysine and arginine), specially so in the tail regions. Conversely, DNA is a mostly negative molecule due to its negatively charged phosphate backbone. The resulting strong electrostatic interactions between histones and DNA lead to the tight packing of DNA inside the nucleus. Although DNA compaction is an absolute logistical requirement for eukaryotic cells (the unwound human genome is about 2 m long), it also imposes accessibility constraints on the transcriptional machinery. To circumvent this limitation, histone acetylation has evolved so as to allow the spatial and temporal regulation of chromatin unpacking, thus enabling the transcriptional machinery to access specific DNA templates.

Acetylation of histones is a reaction catalyzed by histone acetyl transferases (HATs), which transfer acetyl groups from acetyl coenzyme A (Ac-CoA) to the ε-amino group of conserved lysine residues in histone tails (Fig. 1.4). Although not as common, acetylation of lysine residues in the globular domain of histones is also known to occur (Ozdemir et al., 2006). Neutralization of lysine's positive charge disrupts the electrostatic histone-DNA interactions, promoting the unraveling of chromatin (Kouzarides, 2007). The opposite reaction, performed by histone deacetylases (HDACs), restores lysine's positive charge and promotes chromatin

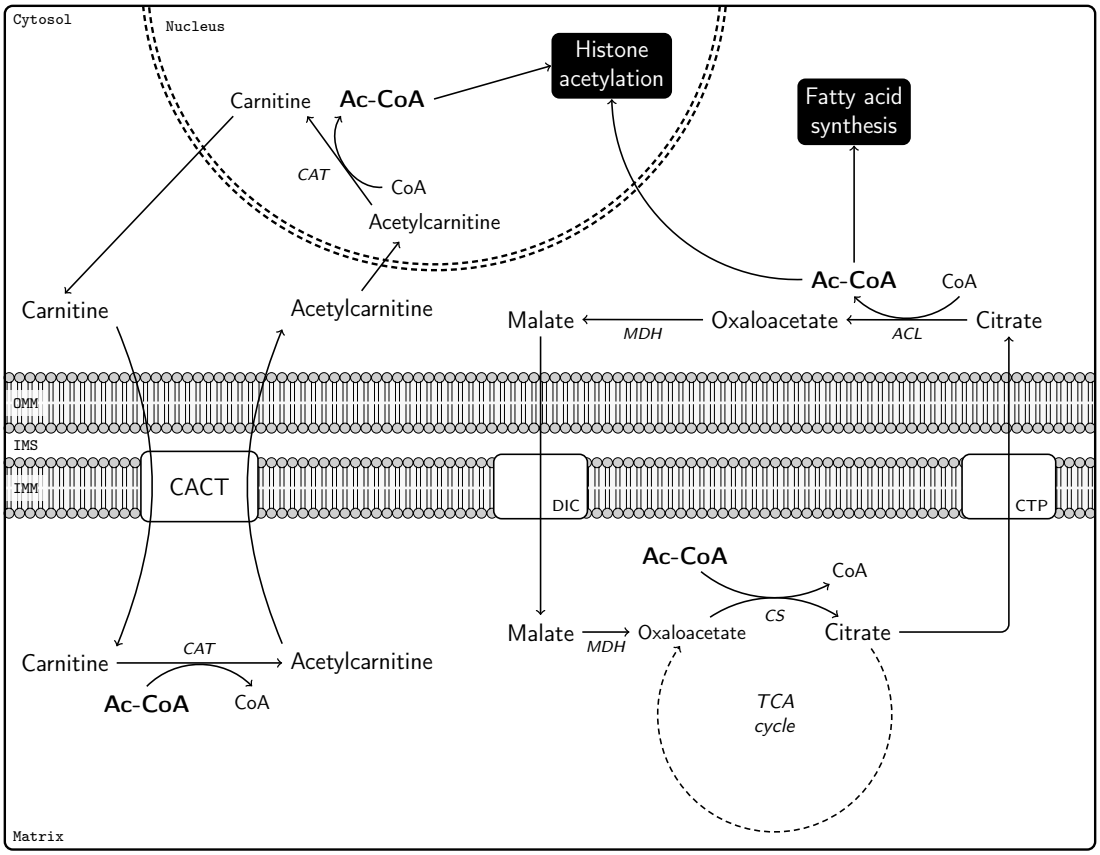

Figure 1.5. Overview of the citrate and the carnitine shuttles. The carnitine shuttle is illustrated as being unidirectional for simplicity, but the system is fully reversible. Conversely, the citrate shuttle is an irreversible system. Abbreviations: CS, citrate synthase; CTP, citrate transport protein; DIC, dicarboxylate ion carrier; IMM, inner mitochondrial membrane; IMS, intermembrane space; MDH, malate dehydrogenase; OMM, outer mitochondrial membrane. Other abbreviations are described in the text.

condensation. The overall steady-state equilibrium of histone acetylation is determined by the dynamic, opposing activities of histone acetyltransferases and deacetylases.

Acetyl coenzyme A

Acetyl coenzyme A is a central metabolite found at the crossroads of multiple metabolic pathways. It is mainly generated in the mitochondrial matrix from pyruvate and free fatty acids (FFAs), via the activities of pyruvate dehydrogenase (PDH) and the β-oxidation pathway, respectively. Peroxisomes can also generate Ac-CoA via β-oxidation, but the relative contribution of this organelle in cardiac tissue is believed to be insignificant (Chu et al., 1994).

Because the mitochondrial inner membrane is impermeable to Ac-CoA, the acetyl moieties must be exported to the cytosol by means of a shuttle system in order to be used by cytosolic acetyltransferases. Acetyl groups can leave mitochondria in the form of citrate and acetylcarnitine, via the citrate and carnitine shuttles, respectively (Fig. 1.5). In the citrate shuttle, mitochondrial

citrate generated in the TCA cycle is carried to the cytosol via citrate transport protein (CTP) and is then converted to oxaloacetate by ATP citrate lyase (ACL), generating Ac-CoA in the process. The carnitine shuttle is most commonly implicated in transporting long-chain FFAs into mitochondria for β-oxidation. However, it has also been proposed to act as a buffer system to prevent fluctuations in the mitochondrial Ac-CoA/CoA-SH ratio that would otherwise affect TCA cycle dynamics (Bremer, 1983). The key proteins in the carnitine shuttle are carnitine acetyltransferase (CAT), which interconverts Ac-CoA and acetylcarnitine, and carnitine–acylcarnitine translocase (CACT), which transports carnitine and acetylcarnitine across the mitochondrial inner membrane.

Recent studies in mammalian cells suggest that histone acetylation is linked to mitochondrial-derived Ac-CoA via both the citrate and the carnitine shuttle systems. Thompson and colleagues (Wellen et al., 2009) demonstrated that histone acetylation was dependent on both glucose availability and ACL activity; simultaneously linking the energetic status of the cell and mitochondrial metabolism to epigenetic modulation. In the same year, Madiraju et al. (2009) assessed the effect of L-carnitine and sulfobetaine 3-08 (an inhibitor of mitochondrial carnitine transport) supplementation in histone acetylation levels. The authors reported that L-carnitine supplementation increased histone acetylation levels, and that this effect was abolished by carnitine transport inhibition. The authors also demonstrated the existence of a nuclear CAT, further reinforcing the importance of the carnitine shuttle as a donor of mitochondrial acetyl groups for nuclear acetylation reactions. Furthermore, a series of studies from the '70s in perfused rat hearts suggest that the mitochondrial and cytosolic ratios of Ac-CoA/CoA-SH and carnitine/acetylcarnitine maintain their equilibriums under variable work loads (Oram et al., 1973; Oram et al., 1975; Idell-Wenger et al., 1978), underscoring the carnitine-mediated link between both pools of acetyl groups. Thus, alterations in mitochondrial Ac-CoA pools will likely reflect on the nuclear Ac-CoA pools, thereby conditioning histone acetylation dynamics.

By disrupting overall mitochondrial metabolism, DOX can be expected to interfere with the cellular pools of acetyl groups. Indeed, it was found that DOX treatment leads to greatly elevated Ac-CoA/CoA-SH ratios in mitochondria isolated from rat heart (Ashour et al., 2012). This can be detrimental to cardiomyocyte lipid metabolism for two reasons. First, high Ac-CoA/CoA-SH ratios inhibit the β-oxidation pathway by allosterically inhibiting 3-ketoacyl-CoA thiolase (the final enzyme in the β-oxidation cycle) (Schulz, 2002). Second, excess Ac-CoA will overload the carnitine buffering system, resulting in high acetylcarnitine/carnitine ratios. This limits lipid transport across the mitochondrial inner membrane, as lower levels of free carnitine are available to participate in this process.

It has recently been proposed that mitochondrial Ac-CoA levels couple cellular energetics to nuclear gene transcription regulation (Wallace and Fan, 2010); meaning that high levels of Ac-CoA will invoke a fed state transcriptome via epigenetic modulation. This could explain, at least in part, the overexpression of glycolytic genes in cardiomyocytes exposed to DOX. It would also imply that cells would have to respond to mixed signals regarding their energetic status – low ATP levels would signal for a fasting state whereas high Ac-CoA levels would signal

for an artificial fed state. This pseudo-energy surplus signaling can be further exacerbated by the impairment of the energy sensor AMP-activated protein kinase (AMPK) that has been shown to follow DOX treatment (Tokarska-Schlattner et al., 2005). Clearly, the cardiac metabolic remodeling induced by DOX is a multifactorial process. It remains to be seen to which extent this effect is mediated by aberrant histone acetylation dynamics.

1.2.2 DNA methylation

DNA methylation consists in the addition of a methyl group to the 5 position of cytosine, forming 5-methylcytosine (m^5C) (Fig. 1.6). This modification occurs primarily in CpG dinucleotides, so as to ensure that methylation patterns can be mirrored in both strands of DNA after replication. During DNA synthesis, only unmethylated cytosines are added to the growing strand. The maintenance of the methylation pattern depends on the activity of DNA methyltransferase (DNMT) 1, which binds preferentially to hemimethylated DNA (that is, a m^5CpG dinucleotide that is paired to a GpC dinucleotide)

$$\begin{array}{l} \overset{m^5}{} \\ \texttt{5'-CG-3'} \\ \texttt{3'-GC-5'} \end{array}$$

and catalyzes the symmetrical methylation of the newly added cytosine in the opposing GpC dinucleotide (hence the CpG specificity),

$$\begin{array}{l} \overset{m^5}{} \\ \texttt{5'-CG-3'} \\ \texttt{3'-GC-5'} \\ \quad\quad m^5 \end{array}$$

thus providing a way to propagate methylation patterns between cell generations (Jeltsch, 2006). Unlike DNMT1, both DNMT3a and DNMT3b methylate CpG dinucleotides with no preference for hemimethylated DNA (Okano et al., 1998). De novo methylation by the *Dnmt3* family is essential for the establishment of mammalian embryonic methylation patterns (Okano et al., 1999).

DNA regions with a high CpG density – the so-called "CpG islands" – colocalize frequently with gene promoters or other regulatory regions required for gene transcription, and are mostly unmethylated (Guibert and Weber, 2013). Initially, DNA methylation was described as a repressive mark, since many mammalian transcription factors bind to CpG motifs. Methylation of these motifs prevents the binding of several transcription factors, thus repressing gene expression (Bird and Wolffe, 1999). Recently, however, the outcome of DNA methylation is increasingly being regarded as being context-dependent. Methylation of micro RNA promoter regions is a particular example of how this epigenetic mark can lead to gene expression activation, and has been shown to be an important mechanism in mouse embryonic development (Cui et al., 2009).

Until recently, DNA methylation was believed to be a phenomenon exclusive to nuclear DNA (nDNA). Studies performed in the last few years, however, demonstrate not only the presence of m^5C in mtDNA but also a possible mitochondrial of

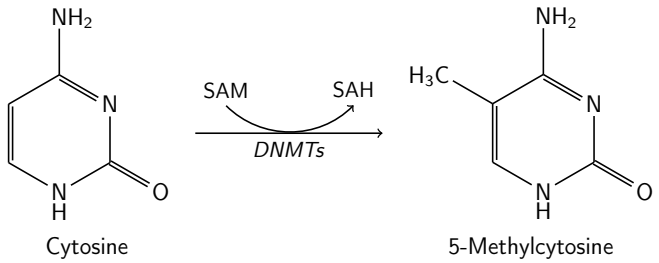

Figure 1.6. DNA methylation mechanism. The DNMT-catalyzed reaction consists in the transfer of a methyl moiety from the universal methyl donor SAM to the 5 position of a cytosine in a CpG dinucleotide.

DNMT1 and DNMT3a in mitochondria (Chestnut et al., 2011; Shock et al., 2011). The field of mtDNA methylation remains remarkably unexplored nonetheless.

S-Adenosyl-L-methionine

The process of DNA methylation requires the universal methyl donor *S*-adenosyl-L-methionine (SAM), which is synthesized through the coordinated activities of the methionine cycle and the folate cycle (Fig. 1.7). SAM is produced in the methionine cycle, where the enzyme methionine adenosyltransferase (MAT) catalyzes the addition of methionine to the adenosyl moiety of ATP, thereby generating SAM. Removal of the methyl group in SAM by various methyltransferases produces *S*-adenosyl-L-homocysteine (SAH), which is hydrolyzed to homocysteine (Hcy) by SAH hydrolase (SAHH). The next step completes the methionine cycle and merges with the folate cycle; methionine synthase (MS) tranfers the methyl group from 5-methyl-tetrahydrofolate (5-MTHF) to Hcy, thus regenerating methionine and producing tetrahydrofolate (THF) as a byproduct (Iacobazzi et al., 2013). The synthesis of methionine – and SAM, by extension – is therefore dependent on a steady supply of 5-MTHF by the folate cycle.

Folate metabolism – also referred to as the one-carbon metabolism – is semi-duplicated in the cytoplasm and in mitochondria. The two compartments carry out folate metabolism for different purposes using parallel, but distinct enzymes. In the cytoplasm, folates donate one-carbon units to the synthesis of thymidylate (dTMP), purines and methionine. Mitochondrial folates are used to generate glycine, *N*-formylmethionyl-tRNA (fMet-tRNA) and to donate one-carbon units for cytoplasmic one-carbon metabolism in the form of formate (Fox and Stover, 2008). Cytoplasmic and mitochondrial folate pools do not equilibrate with each other, but they exchange one-carbon units in the form of serine, glycine and formate (Depeint et al., 2006).

The proper folate metabolism requires some degree of coordination between the two compartments. Imbalances between the two pools may arise from mitochondrial dysfunction. For instance, mitochondrial folate metabolism is strongly influenced by the NADH/NAD^+ ratio. Conversion of THF to methylene-THF in mitochondria can be achieved by redox-coupled reactions, which are performed by NAD^+-dependent dehydrogenases, and by a non-redox-coupled reaction (Fig. 1.7).

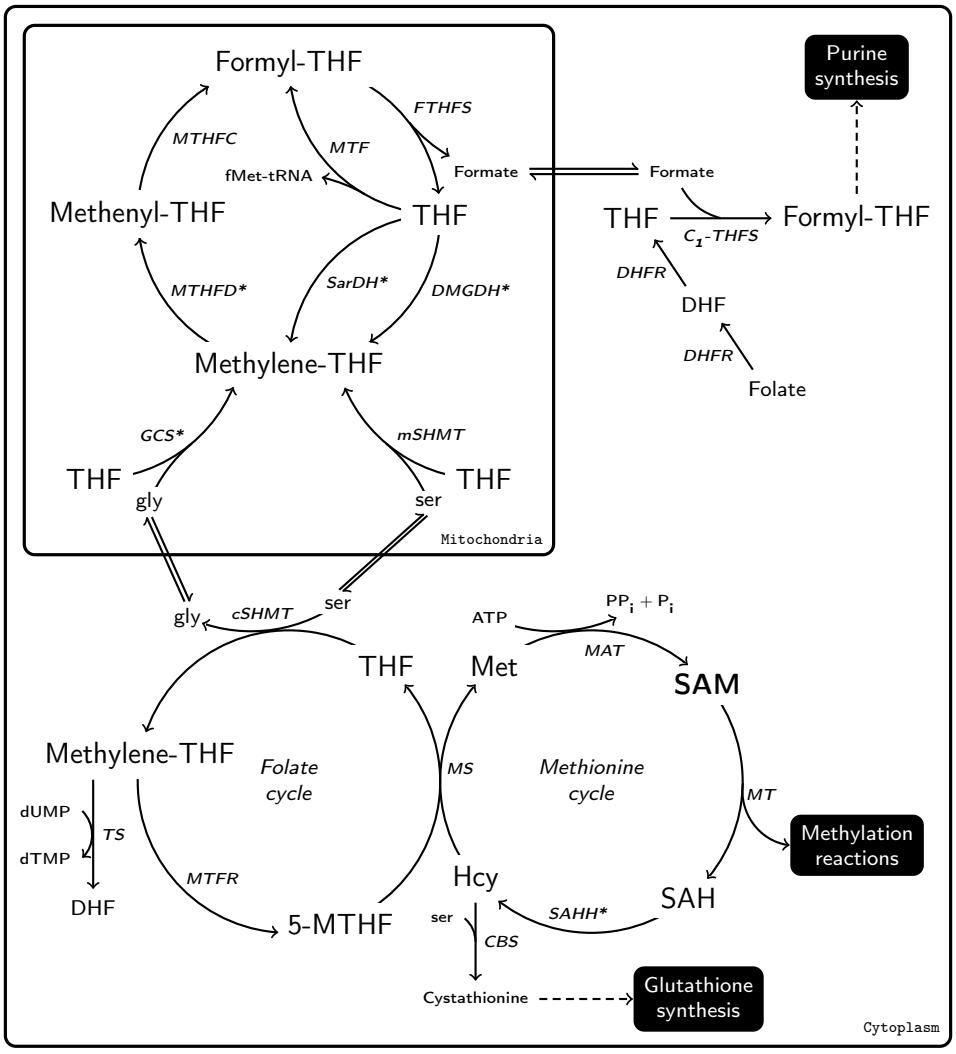

Figure 1.7. Simplified overview of folate-mediated one-carbon metabolism. The connection between methionine metabolism and glutathione biosynthesis is also shown. Asterisks denote NAD(P)$^+$-dependent enzymes. Abbreviations: C_1-THFS, C_1-THF synthase; CBS, cystathionine β-synthase; DHF, dihydrofolate; DHFR, DHF reductase; DMGDH, dimethylglycine dehydrogenase; FTHFS, formyltetrahydrofolate synthetase; GCS, glycine cleavage system; MFT, methionyl-tRNA$_f^{Met}$ formyltransferase; MT, generalized methyltransferase; MTFR, methylene-THF reductase; MTHFC, methenyl-THF cyclohydrolase; MTHFD, methylene-THF dehydrogenase; SarDH, sarcosine dehydrogenase; TS, thymidylate synthase. Other abbreviations are described in the text.

Impairment of the ETC decreases the mitochondrial oxidation of NADH to NAD$^+$, thus increasing the NADH/NAD$^+$ ratio. This limits the entry of THF into the mitochondrial folate cycle via redox-coupled reactions, forcing mitochondria to rely primarily on one-carbon units from serine via the activity of mitochondrial serine hydroxymethyl transferase (mSHMT). As a result, cytosolic serine is transfered to mitochondria to support mitochondrial folate metabolism, slowing down in turn cytoplasmic folate metabolism at the cytosolic serine hydroxymethyl transferase (cSHMT) step. This has a propagating effect in the methionine cycle by hindering the cytoplasmic folate cycle, thus decreasing the pools of 5-MTHF that feed the

synthesis of methionine (Naviaux, 2008). Evidence in favor of this reasoning comes from an in vitro study using ρ^0 cells, which are devoid of mtDNA (Smiraglia et al., 2008). Depletion of mtDNA compromises OxPhos metabolism since mtDNA encodes for 11 subunits of the ETC complexes (I, III and IV) and 2 subunits of ATP synthase (Taanman, 1999). The authors reported significant alterations in the methylation patterns of several genes, which were only partially reversed upon re-introduction of wild-type mitochondria.

An alternative route to divert substrates away from the methionine cycle is the glutathione (GSH) biosynthetic pathway. De novo synthesis of GSH requires cysteine, which can be derived from Hcy and serine in the transsulfuration pathway (Lu, 2009). Depletion of GSH pools by excessive oxidative stress increases the flux of Hcy to the GSH biosynthetic pathway, thus diverting Hcy and serine away from the methionine salvage pathway and the cytoplasmic folate cycle, respectively.

Doxorubicin can be expected to interfere with SAM metabolism by both mechanisms discussed above. Increases in the NADH/NAD^+ ratio would arise from ETC impairment due to protein carbonylation and mtDNA oxidation. Two recent studies, one using an in vitro model (Wang et al., 2012) and the other a perfused heart system (Montaigne et al., 2010), provide indirect evidence that DOX increases the NADH/NAD^+ ratio in cardiomyocytes. Depletion of GSH would result from excessive oxidative stress; such has been shown to occur in cardiac tissue of rats treated with DOX (Zhou et al., 2001b; Sadik et al., 2008). Interestingly, a study from the early '90s reported a significant protective effect in DOX-treated rats that were co-administered SAM (Russo et al., 1994). However, whether this effect is due to epigenetic maintenance, increased GSH levels or some other factor remains to be investigated.

1.3 Objectives

The molecular connection between cellular metabolism and epigenetic modifications has been discussed above and is summarized in Fig. 1.8. Given that DOX disrupts normal cardiomyocyte metabolism, the overall hypothesis behind this project is that DOX disturbs the pool of metabolites directly or indirectly involved in epigenetic modulation, thereby altering normal cardiomyocyte epigenetic patterns in a non-reversible manner upon withdrawal of the drug and ultimately locking the cardiomyocyte in a pathological transcriptional phenotype. This would account for many observations described in the literature and indeed for the persistent nature of DOX-induced cardiotoxicity.

Having in mind the background described and our general hypothesis, the objective of the present work is to verify if there is a correlation between mitochondrial dysfunction, epigenetic disruption and alteration to the transcriptome – all of which are necessary to be in place to corroborate our general and more far-reaching hypothesis.

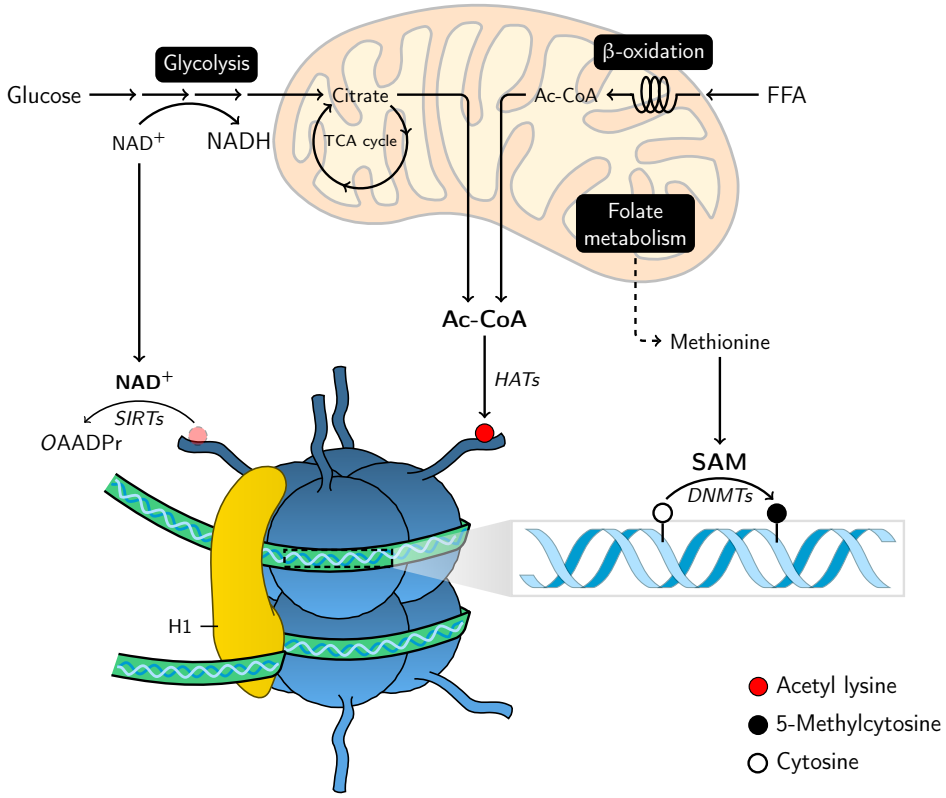

Figure 1.8. Relationship between cellular metabolism and epigenetic modifications. The glycolytic flux affects the NADH/NAD^+ ratio, which controls the activity of sirtuin histone deacetylases. Mitochondrial citrate and Ac-CoA levels determine the levels of cytosolic Ac-CoA that is used as an acetyl donor for HAT-mediated histone acetylation. Finally, the synthesis of SAM, the methyl donor for DNMT-mediated DNA methylation, is dependent on the metabolism of methionine, which in turn is indirectly regulated by mitochondrial folate metabolism. Abbreviations: H1, histone H1; *O*AADPr, *O*-acetyl-ADP ribose. Other abbreviations are described in the text.

Chapter 2

Materials and Methods

2.1 Animals and treatment protocol

Male Wistar Han rats were purchased form Charles River Laboratories (France) with 7 weeks of age. One week prior to the initiation of the experiment, animals were acclimated and maintained in local animal house facilities (CNC – Faculty of Medicine, University of Coimbra, Coimbra, Portugal). Animals were group-housed in type III-H cages (Tecniplast, Italy) with irradiated corn cob grit bedding (Scobis Due, Mucedola, Italy) and environmental enrichment, maintained in controlled environmental requirements (22 °C, 45–60 % humidity, 15–20 air changes/hour, 12 hours artificial light/dark cycle, noise level < 55 dB) and free access to standard rodent food (4RF21 GLP certificate, Mucedola, Italy) and HCl-acidified water (pH 2.6).

Experimental manipulation was initiated with 8 weeks old rats weighing 220–260 g. Animals were randomly assigned to two experimental groups: saline (SAL)-treated ($n = 6$) and DOX-treated ($n = 6$). Rats received seven weekly subcutaneous injections of DOX ($2\,\mathrm{mg\,kg^{-1}}$), dissolved in normal saline (0.9 % [w/v] NaCl), or an equivalent volume of SAL solution. All animals were injected and weighed during the light phase of the cycle. Animals were euthanized by cervical dislocation followed by decapitation two weeks after the last injection (Fig. 2.1). *

2.2 Subcellular fractionation

Subcellular fractions for Western blotting analyses were obtained from heart and liver tissue according to the method described by Dimauro et al. (2012), with slight modifications. The procedure is summarized in Fig. 2.2. Excised tissue was weighed (20 mg), rinsed with PBS, resuspended in ice-cold sucrose-Tris-magnesium (STM) buffer (50 mM Tris-HCl [pH 7.4], 250 mM sucrose, 50 mM $MgCl_2$; supplemented freshly with 1 mM dithiothreitol [DTT], $1\,\mu\mathrm{L\,mL^{-1}}$ protease inhibitor cocktail

*The animal treatment protocol and animal data shown in Fig. 3.1 and Table 3.1 was performed by Filipa S. Carvalho (FELASA category B accredited), Ana Burgeiro and Rita Garcia.

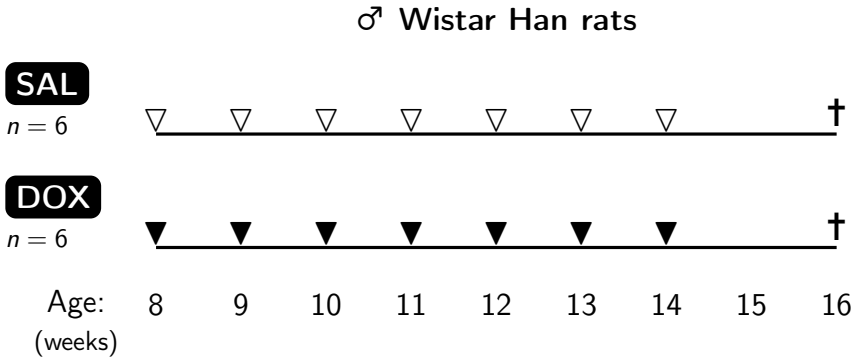

Figure 2.1. Timeline of the treatment protocol. Animals were given seven weekly subcutaneous injections of DOX ($2\,\mathrm{mg\,kg^{-1}}$; ▼) or of SAL solution (▽). All animals were euthanized at 16 weeks of age (†).

[PIC; Sigma–Aldrich, Barcelona, Spain; #P8340], 5 mM nicotinamide [NAM] and 5 mM sodium butyrate [SB]) and homogenized on ice in a pre-cooled Potter–Elvehjem glass homogenizer using a tight-fitting Teflon pestle (wall clearance: 0.10 mm) attached to a mechanical overhead stirrer (Heidolph, Germany) set to 600 rpm for 50–60 strokes. The homogenate was decanted into a microcentrifuge tube and maintained on ice for 15 min, vortexed at maximum speed for 15 s and centrifuged at 800 *g* for 15 min at 4 °C. The supernatant was labeled as S_1 and used for concurrent extraction of cytosolic and mitochondrial fractions. The pellet was washed thrice with centrifugation steps after resuspension in STM buffer. The washed pellet was then resuspended in NaCl-EDTA-HEPES (NEH) buffer (0.5 M NaCl, 0.2 mM EDTA, 20 mM HEPES, pH 7.9, 1.5 mM $MgCl_2$, 20 % [v/v] glycerol, 1 % [v/v] Triton X-100; supplemented as before) , vortexed at maximum speed for 15 s and maintained on ice for 30 min. Nuclei were lysed with sonication (3× in 10 s bursts) in a water bath sonicator with 30 s pauses between sonication steps whilst keeping on ice throughout. The lysate was centrifuged for 30 min at 9,000 *g* and the resulting supernatant (the nuclear fraction) was stored at −80 °C until use.

Concurrently, cytosolic and mitochondrial fractions were obtained from the supernatant S_1 by centrifugation at 800 *g* for 10 min, so as to remove any remaining nuclear contamination. If the nuclear pellet P_2 was substantial, it was resuspended in STM buffer and combined with the pellet $P_{1.1}$. The supernatant S_2 containing the cytosolic and mitochondrial fractions was centrifuged for 10 min at 11,000 *g*, the supernatant S_3 was precipitated in cold 80 % acetone supplemented with 1 M NaCl at −20 °C for 1 h (Crowell et al., 2013) and subsequently centrifuged for 10 min at 11,000 *g*. The resulting pellet P_4 (the cytosolic fraction) was resuspended in STM buffer and stored at −80 °C until use. The mitochondrial pellet $P_{3.1}$ was washed once with a centrifugation step after resuspension in STM buffer, the washed pellet was then resuspended in Tris-EDTA with Triton X-100 (TE-$T_{X\text{-}100}$) buffer (50 mM Tris-HCl [pH 6.8], 1 mM EDTA, 0.5 % [v/v] Triton X-100; supplemented as before), sonicated as before and stored at −80 °C until use.

Nuclear fractions for enzymatic activity assays were obtained from heart and

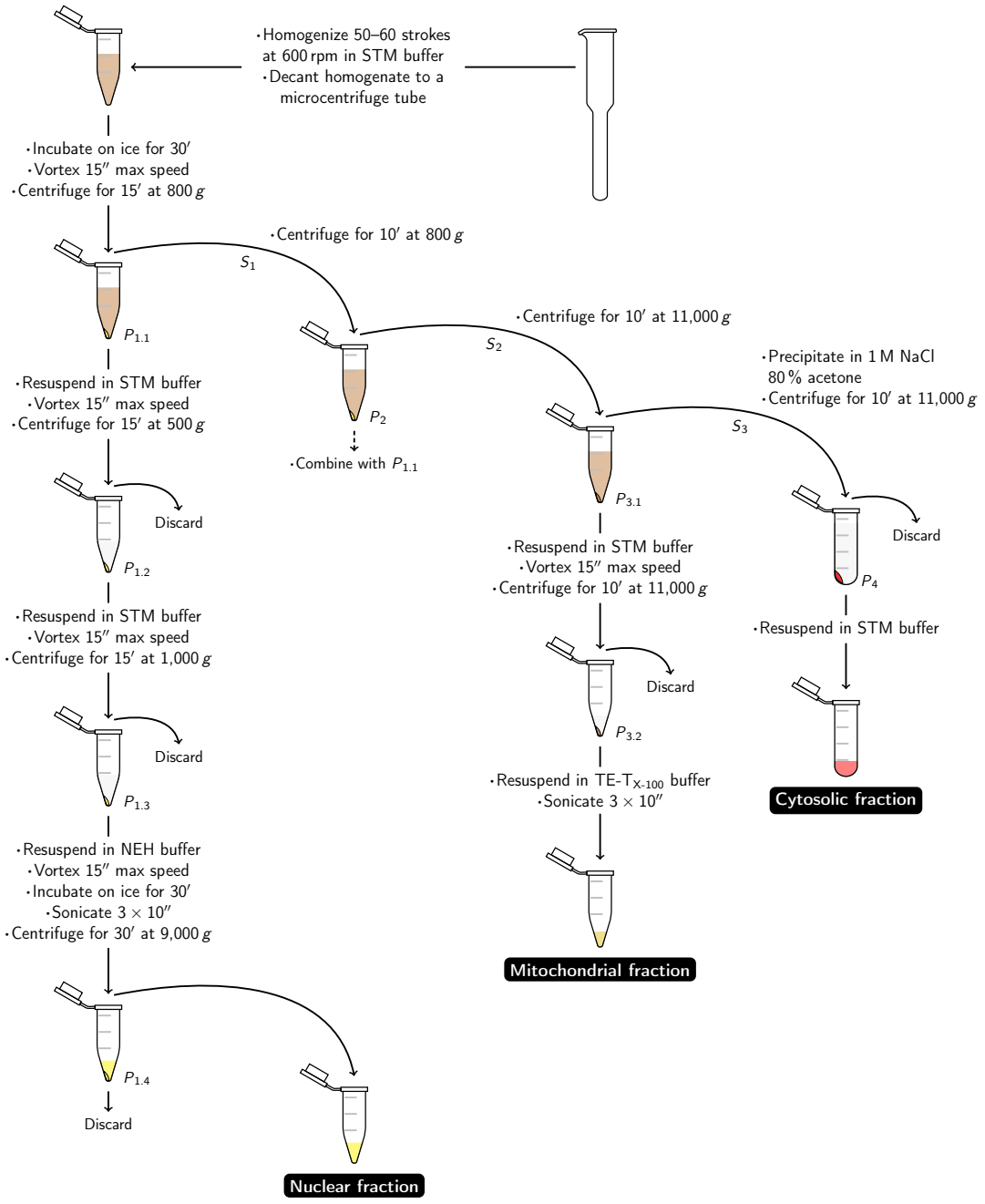

Figure 2.2. Schematic workflow of the subcellular fractionation protocol. The dashed arrow denotes an optional step.

liver tissue as described above, but with the omission of buffer supplementation. Protein content of all extracts was determined by the BCA assay, calibrated with bovine serum albumin.

2.3 DNA extraction

Total genomic DNA for mtDNA and m^5C quantification was extracted from heart and liver tissue using the PureLink™ Genomic DNA Mini Kit (Invitrogen), according to the manufacturer's instructions. Briefly, excised tissue was weighed (15–20 mg) and incubated with digestion buffer and proteinase K (NZYTech, Portugal; `MB01902`). The lysate was centrifuged and the resulting supernatant was treated with RNase A. After incubation, the lysate was mixed with binding buffer and ethanol and centrifuged through a silica-based spin column. After washing the column, bound DNA was eluted by centrifuging elution buffer through the column. The extracted DNA samples were quantified spectrophotometrically at $A_{260\,nm}$ using a NanoDrop 2000 spectrophotometer (Thermo Scientific, USA) and stored at −80 °C until use.

2.4 RNA extraction and cDNA synthesis

Total RNA was extracted from heart and liver tissue using the Aurum™ Total RNA Mini Kit (Bio-Rad, Hercules, CA, USA), according to the manufacturer's specifications. Briefly, excised tissue was weighed (15–20 mg) and immediately homogenized in lysis solution using a T 25 Ultra-Turrax® dispersion device (IKA®, Germany). After centrifuging the lysate at 16,000 *g* for 3 min, the resulting supernatant was diluted 1:1 with 60 % ethanol and centrifuged through a silica-based spin column at 16,000 *g* for 1 min. Following a washing step, the column was incubated with DNase I for 25 min at room temperature. Additional washing steps were performed before the column-bound RNA was eluted by centrifuging the provided elution solution through the column. Thereafter, RNA quality and integrity was ascertained by visualization of the 18 S/28 S rRNA band pattern using an Experion™ Automated Electrophoresis System (Bio-Rad). Total RNA was quantified spectrophotometrically at $A_{260\,nm}$ using a NanoDrop 2000 spectrophotometer (Thermo Scientific) and stored at −80 °C until use.

First-strand complementary DNA (cDNA) synthesis was performed using the iScript™ cDNA synthesis kit (Bio-Rad), according to the manufacturer's specifications. Briefly, oligo(dT)/random hexamer primer mediated reverse transcription was carried out in reactions comprising 1 µg of total RNA, 1× iScript™ reaction mix and iScript™ reverse transcriptase, made up to 20 µL with nuclease-free water, under the following cycling parameters:

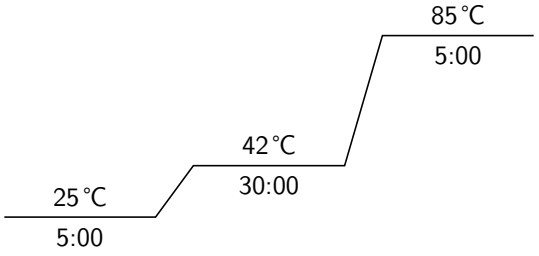

2.5 HAT activity assay

Histone acetyltransferase activity in cardiac and liver tissue was measured using the colorimetric Histone Acetyltransferase Assay Kit (Abcam; `ab65352`), according to the manufacturers' instructions. This kit measures the acetylation rate of a peptide substrate by active HATs. This process releases free CoA, which then serves as a coenzyme for the production of NADH by a NADH-generating enzyme (undisclosed). The rate of NADH production is measured spectrophotometrically through the reduction of a tetrazolium salt into a colored formazan product. Briefly, 25 µg of nuclear extract were incubated with HAT substrates I and II and NADH-generating enzyme in assay buffer for 2 h at 37 °C. Absorbance was measured at 440 nm using a Cytation™ 3 microplate reader (BioTek, USA).

2.6 HDAC activity assay

Histone deacetylase activity in cardiac tissue was measured using the fluorimetric Histone Deacetylase Activity Assay Kit (Abcam; `ab156064`), according to the manufacturers' instructions. This kit measures the deacetylation rate of a fluorescence-labeled acetylated peptide substrate by active HDACs.

$$\mathrm{X{-}X{-}X{-}(Ac)K{-}MCA} \xrightarrow[\mathrm{H_2O}]{HDACs} \mathrm{X{-}X{-}X{-}K{-}MCA} + \mathrm{AcOH} \qquad \{2.1\}$$

Upon deacetylation, the substrate peptide is cleaved by a peptidase (lysyl endopeptidase, LE)

$$\mathrm{X{-}X{-}X{-}K{-}MCA} \xrightarrow{LE} \mathrm{X{-}X{-}X{-}K} + \mathrm{AMC} \qquad \{2.2\}$$

and the fluorescent group (7-amino-4-methyl coumarin, AMC) is released. The measured fluorescence is directly proportional to the activity of HDACs. The specificity of the assay was ascertained with negative controls containing trichostatin A – a selective inhibitor of class I and II HDACs. Briefly, 25 µg of nuclear extract were incubated with the substrate peptide and endopeptidase in assay buffer for 30 min at room temperature. Fluorescence was measured at $\lambda_{\mathrm{Ex}}/\lambda_{\mathrm{Em}} = 355/460$ nm using a Cytation™ 3 microplate reader (BioTek, USA).

2.7 Enzyme-linked immunosorbent assay (ELISA) of global DNA $\mathrm{m^5C}$ content

The $\mathrm{m^5C}$ content of total DNA from heart and liver tissue was determined using the fluorometric EpiSeeker Methylated DNA Quantification Kit (Abcam; `ab117129`), according to the manufacturer's instructions. Briefly, 100 ng of DNA were bound to the provided assay wells, incubated for 60 min with capture antibody and then for 30 min with detection antibody. After incubating the probed DNA with the provided substrate for 4 min, methylated DNA was quantified fluorimetrically by reading the fluorescence at $\lambda_{\mathrm{Ex}}/\lambda_{\mathrm{Em}} = 544/590$ nm in a Victor™ *X*3 multilabel plate reader (PerkinElmer). Results were expressed as percent $\mathrm{m^5C}$, calculated using a linear regression equation generated with controls provided in the kit.

2.8 Primer design

Primers used in quantitative real-time PCR for nDNA-encoded gene transcripts were designed using the Primer-BLAST online tool (NCBI) with the following specifications: PCR product size 90–200 bp; exon-exon junction span enforced when possible. For mtDNA genes and respective transcripts, primers were designed using the Beacon Designer™ 8.0 software (Premier Biosoft International). For the nDNA β_2M (*B2m*) gene, primers were designed using Primer-BLAST with the following specifications: PCR product size 90–200 bp; exon-intron junction span enforced. All primer sequences used in this study are shown in Table 2.1.

2.9 Quantitative real-time PCR

Quantitative real-time PCR (qPCR) was performed in duplicate reactions, each comprising 12.5 ng of either cDNA or DNA, 500 nM of each gene-specific primer and 1× SsoFast™ EvaGreen® Supermix (Bio-Rad), made up to 10 µL with nuclease-free water. Reactions were performed in sealed 96-well plates and monitored with a CFX96™ Real-Time PCR Detection System (Bio-Rad). Results were analysed using the CFX Manager™ 3.1 software (Bio-Rad). For gene expression analyses, reactions were performed with the following cycling parameters:

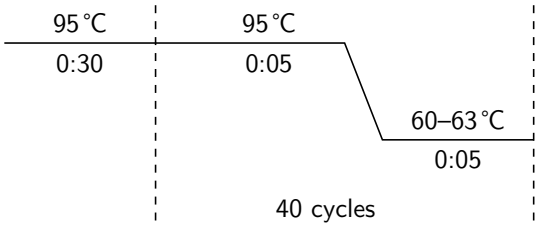

To confirm the absence of genomic DNA contamination, a negative control was included in the reverse transcriptase reaction. Genomic DNA contamination was considered insignificant when the cycle threshold difference between the no-reverse transcriptase and the respective sample was above 10 cycles. Transcript levels were normalized relative to the expression of three housekeeping genes (*18 S* [*Rn18s*], *TBP* [*Tbp*] and *β-actin* [*Actb*]) using the Pfaffl method (Pfaffl, 2001). For mtDNA copy number quantification, reactions were performed with the following cycling parameters:

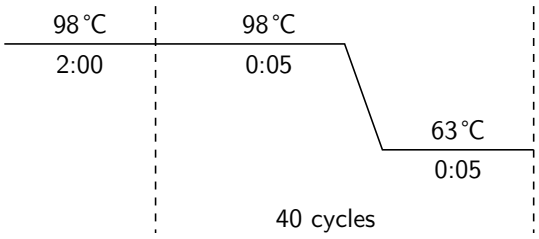

Levels of the mitochondrial *COX1* (*Mt-co1*) gene were normalized relative to the levels of the single-copy nuclear β_2M gene, also using the Pfaffl method. For all reactions, amplification of a single PCR product was confirmed by melt curve

Table 2.1
List of oligonucleotide primer sequences used for qPCR. Symbols and names are relative to the Rat Genome Database (RGD, http://rgd.mcw.edu/); accession numbers are relative to the GenBank® database (Benson et al., 2014). For each primer, F and R indicate forward and reverse orientation, respectively.

Target	Symbol	Name	Accession no.	Sequence
18 S	*Rn18s*	18S ribosomal RNA	NR_046237	F 5'-ACTCAACACGGGAAACCTC-3'
				R 5'-ACCAGACAAATCGCTCCAC-3'
ACAA2	*Acaa2*	acetyl-CoA acyltransferase 2	NM_130433	F 5'-CCTCAGTTCTTGGCTGTTCA-3'
				R 5'-CCACCTCGACGCCTTAAC-3'
ACC2	*Acacb*	acetyl-CoA carboxylase beta	NM_053922	F 5'-ACAGCAAGAGCCTTCAAGAG-3'
				R 5'-CGCAGTCCGTAATCCACAA-3'
ACL	*Acly*	ATP citrate lyase	NM_016987[a]	F 5'-GCTGCGTTACCAAGACACT-3'
				R 5'-AACTGGACCTCAGAAGAGAACA-3'
ACOX1	*Acox1*	acyl-CoA oxidase 1, palmitoyl	NM_017340	F 5'-GCAGACAGCCAGGTTCTTGATG-3'
				R 5'-ACTCGGCAGGTCATTCAGGTAT-3'
ATP8	*Mt-atp8*	mitochondrially encoded ATP synthase 8	AC_000022[b]	F 5'-TGCCACAACTAGACACATCCACAT-3'
				R 5'-GAGGGAGGTGCAGGAAAGGTT-3'
CACT	*Slc25a20*	solute carrier family 25 (carnitine/acylcarnitine translocase), member 20	NM_053965	F 5'-GGAGAACGGATCAAATGCTTACT-3'
				R 5'-GGCAGGAACATCTCGCAT-3'
CBP	*Crebbp*	CREB binding protein	NM_133381	F 5'-GCACCCATGCCAACAACATT-3'
				R 5'-ACCTGGCCCTGTGAAACAC-3'
COX1	*Mt-co1*	mitochondrially encoded cytochrome c oxidase I	AC_000022[b]	F 5'-GCCAGTATTAGCAGCAGGTATCA-3'
				R 5'-GCCGAAGAATCAGAATAGGTGTTG-3'
Cyt b	*Mt-cyb*	mitochondrially encoded cytochrome b	AC_000022[b]	F 5'-TACGCTATTCTACGCTCCATTC-3'
				R 5'-GCCTCCGATTCATGTTAAGACTA-3'
Cyt c	*Cycs*	cytochrome c, somatic	NM_012839	F 5'-CTTGGGCTAGAGAGCGGGAC-3'
				R 5'-CCCATTTTAAATTCGGTCCGGG-3'
DNMT1	*Dnmt1*	DNA (cytosine-5-)-methyltransferase 1	NM_053354	F 5'-GGAAGGTGAGCATCGACGAA-3'
				R 5'-TGCTGTGACCCTGGCTAGAT-3'
Ep300	*Ep300*	E1A binding protein p300	XM_001076610	F 5'-TGGAGGCACTTTACCGACAG-3'
				R 5'-GATCCATGGGGCTCTTCACA-3'

[a] Amplifies other transcript variants.
[b] Reference sequence for the complete Wistar strain mitochondrial genome.

(*continued on next page*)

Table 2.1 (*continued*)

Target	Symbol	Name	Accession no.	Sequence
HDAC1	*Hdac1*	histone deacetylase 1	NM_001025409	F 5'-AGCCAAAGGGGTCAAAGAAGA-3' R 5'-TGAGAAATTGAGGGAAAGTAAGGGA-3'
HDAC2	*Hdac2*	histone deacetylase 2	NM_053447	F 5'-GGAGGTCGTAGGAATGTCGC-3' R 5'-TTTGGCTCCTTTGGTGTCTGT-3'
HDAC3	*Hdac3*	histone deacetylase 3	NM_053448	F 5'-CTGGGAGGTGGTGGTTACAC-3' R 5'-TCTGATTCTCGATGCGGGTG-3'
HDAC4	*Hdac4*	histone deacetylase 4	NM_053449	F 5'-CATGGTTCAACGTTCATCTCTGC-3' R 5'-CGCAAACTCGAAGTCCCACT-3'
HDAC5	*Hdac5*	histone deacetylase 5	NM_053450	F 5'-CCCGTCCGTCTGTCTGTTAT-3' R 5'-CCTGACATGCCATCCGACTC-3'
HDAC6	*Hdac6*	histone deacetylase 6	XM_001057931	F 5'-CCCTACAGGAGGTGGAGTTG-3' R 5'-GCTCCTGGAACGGCTCTTT-3'
HDAC7	*Hdac7*	histone deacetylase 7	XM_001059057	F 5'-GACAAGAGCAAGCGAAGTGC-3' R 5'-ACTGTTCTCTCAAGGGCTGC-3'
HDAC8	*Hdac8*	histone deacetylase 8	NM_001126373	F 5'-GTGCTGGAAATCACGCCAAG-3' R 5'-CACATGCTTCAGATTCCCTTTGA-3'
HDAC9	*Hdac9*	histone deacetylase 9	NM_001200045	F 5'-AAACCCAGCATCTGACCTCCA-3' R 5'-CTGATTTCACGTCCACTGAGCTG-3'
HDAC10	*Hdac10*	histone deacetylase 10	NM_001035000	F 5'-GCCCATAGAGGTCAGAGGAGA-3' R 5'-AGGCTAAGGGCAGTACCAGA-3'
MAT2a	*Mat2a*	methionine adenosyltransferase II, alpha	NM_134351	F 5'-GGGGAAGGTCATCCAGATAAGA-3' R 5'-AGCAACAGTTTCACAAGCCAC-3'
ND1	*Mt-nd1*	mitochondrially encoded NADH dehydrogenase 1	AC_000022[a]	F 5'-TCCTCCTAATAAGCGGCTCCTTCT-3' R 5'-TGGTCCTGCGGCGTATTCG-3'
ND6	*Mt-nd6*	mitochondrially encoded NADH dehydrogenase 6	AC_000022[a]	F 5'-TCCTCAGTAGCCATAGCAGTTGT-3' R 5'-GTTGTCTAGGGTTGGCGTTGAA-3'
NDUFA9	*Ndufa9*	NADH dehydrogenase (ubiquinone) 1 alpha subcomplex, 9	NM_001100752	F 5'-GAGAAGCAAGGCAGTGGGAGAG-3' R 5'-ACGAGAGGCACAGCAAGAAACC-3'

[a]Reference sequence for the complete Wistar strain mitochondrial genome.

(*continued on next page*)

Table 2.1 (*continued*)

Target	Symbol	Name	Accession no.	Sequence
NRF-1	*Nrf1*	nuclear respiratory factor 1	NM_001100708	F 5'-CCAAGCATTACGGACCATAGTT-3' R 5'-CAGTACCAACCTGGATGAGC-3'
NRF-2α	*Gabpa*	GA binding protein transcription factor, alpha subunit	NM_001108841	F 5'-CGGCACCAAGCATATCAC-3' R 5'-GGACCACTGTATAGGATCATAGG-3'
NRF-2β	*Gabpb1*	GA binding protein transcription factor, beta subunit 1	NM_001039036	F 5'-GCACCGCTGTCATTTTGTCG-3' R 5'-CAGAGCAGTCTCACGTCCTC-3'
PCAF	*Pcaf*	p300/CBP-associated factor	XM_003750617	F 5'-CAGGTCAAGGGCTATGGAACC-3' R 5'-CCCATCAAAGTGGCTCCTTCA-3'
PGC-1α	*Ppargc1a*	peroxisome proliferator-activated receptor gamma, coactivator 1 alpha	NM_031347	F 5'-TGAGAAGCGGGAGTCTGAAAG-3' R 5'-AACCATAGCTGTCTCCATCATCC-3'
POLγ	*Polg*	polymerase (DNA directed), gamma	NM_053528	F 5'-ATAATGGCCCACACCCGTTT-3' R 5'-GAGTTTCCGGTACCACCCAG-3'
PPARα	*Ppara*	peroxisome proliferator activated receptor alpha	NM_013196	F 5'-AGACTAGCAACAATCCGCCTTT-3' R 5'-TGGCAGCAGTGGAAGAATCG-3'
SDHA	*Sdha*	succinate dehydrogenase complex, subunit A, flavoprotein (Fp)	NM_130428	F 5'-CTATGGAGACCTACAGCATCT-3' R 5'-AATCCGCACCTTGTAATCTTC-3'
TAZ	*Taz*	tafazzin	NM_001025748	F 5'-CAAATGGGGAATTGGACGGC-3' R 5'-AGGGAGTGTACTGAAGGGCT-3'
TBP	*Tbp*	TATA box binding protein	NM_001004198	F 5'-CCTATCACTCCTGCCACACC-3' R 5'-CAGCAAACCGCTTGGGATTA-3'
TFAM	*Tfam*	transcription factor A, mitochondrial	NM_031326	F 5'-AATGTGGGGCGTGCTAAGAA-3' R 5'-TCGGAATACAGATAAGGCTGACAG-3'
UQCRC1	*Uqcrc1*	ubiquinol-cytochrome c reductase core protein I	NM_001004250	F 5'-GAGACACAGGTCAGCGTATTG-3' R 5'-TTTGTTCCCTTGAAAGCCAGAT-3'
UQCRFS1	*Uqcrfs1*	ubiquinol-cytochrome c reductase, Rieske iron-sulfur polypeptide 1	NM_001008888	F 5'-GGACGTGAAGCGACCCTT-3' R 5'-CGAACAGAAGCAGGAACATTCAG-3'
β_2M	*B2m*	beta-2 microglobulin	24223[a]	F 5'-AGAGAACTCAACGGTGGCA-3' R 5'-CGACCGCACACTATAGGGAC-3'
β-actin	*Actb*	actin, beta	NM_031144	F 5'-AGATCAAGATCATTGCTCCTCCT-3' R 5'-ACGCAGCTCAGTAACAGTCC-3'

[a]Gene ID.

analyses and PCR product 2 % agarose gel electrophoresis at the end of every experiment. *

2.10 Mitochondrial DNA integrity

mtDNA integrity was evaluated with a PCR-based assay adapted from Kovalenko and Santos (2009) and Bliksoen et al. (2015). The rationale for this assay is based on the ability of some lesions (e.g. single- and double-strand breaks) to block the progression of the polymerase on DNA templates, resulting in decreased amplification of the target amplicon. Assuming a Poisson distribution, which models that DNA lesions are randomly distributed, amplification of long templates is selectively inhibited, since short templates have a lower probability of having lesions and are therefore considered as representative of undamaged DNA. Because only a single lesion per strand is necessary to block the polymerase, the ratio between a long fragment and a short fragment effectively measures the fraction of undamaged template molecules.

Two separate PCR reactions were performed – one amplifying a long 10,821 bp (10 kb) fragment of mtDNA and the other amplifying a short 121 bp fragment of mtDNA. For the 10 kb fragment, primer sequences used were the forward and reverse primers of the *ND1* (*Mt-nd1*) and *ND6* (*Mt-nd6*) targets, respectively (see Table 2.1). PCR was performed in reactions comprising 50 ng of total DNA, 500 nM of each primer and 1× Phusion™ Hot Start II High-Fidelity PCR Master Mix (Thermo Scientific), made up to 25 µL with nuclease-free water, under the following cycling parameters:

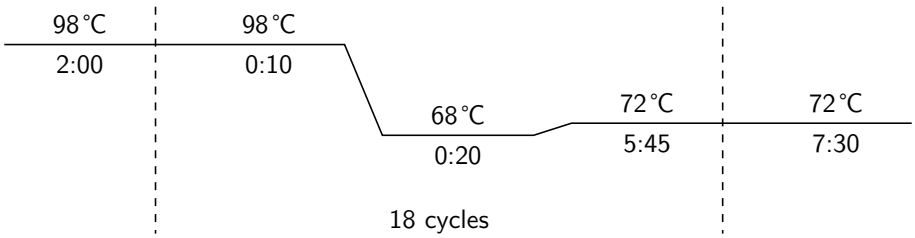

For the 121 bp fragment, primer sequences used were the forward and reverse primers of the *COX1* target (see Table 2.1). PCR was performed in reactions comprising 50 ng of total DNA, 500 nM of each primer and 1× HotStarTaq® Master Mix (Qiagen, Germany), made up to 25 µL with nuclease-free water, under the following cycling parameters:

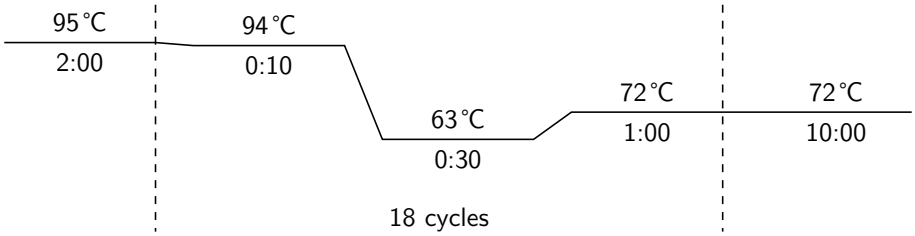

*Andreia Vilaça assisted with qPCR experiments.

For both fragments, a control reaction containing 50 % (25 ng) of total DNA was included to confirm that the PCR was terminated in the exponential phase. After diluting the 10 kb and 121 bp PCR mixtures in loading buffer (2.5 % [w/v] Ficoll 400), equivalent volumes of the diluted mixtures (5 µL) alongside 1 kb and 100 bp DNA ladders were loaded onto 0.7 % and 2 % agarose gels stained with GreenSafe Premium (NZYTech; `MB13201`) and separated electrophoretically at 100 V for 30 min. After the run, gels were imaged using a Benchtop UV Transilluminator (UVP, LLC Upland, CA, USA; Cambridge, UK) and a BioSpectrum® 500 imaging system (UVP). PCR products were quantified by densitometric scanning as detailed below. mtDNA integrity was determined by calculating the ratio between the 10 kb fragment and the 121 bp fragment.

2.11 Western blotting

Subcellular fractions from ventricular heart tissue, obtained as described above, were denatured in Laemmli sample buffer (60 mM Tris-HCl [pH 6.8], 2 % [w/v] SDS, 10 % [v/v] glycerol, 100 mM DTT, 0.01 % [w/v] bromophenol blue) at 95 °C for 5 min. Equivalent amounts of protein (15 µg) alongside a pre-stained protein marker of known molecular weight (NZYTech; `MB09002`) were loaded onto 10 %, 1.5 mm handcast SDS-PAGE gels and separated electrophoretically at a constant voltage of 120 V until the bromophenol blue dye front reached the bottom of the gel. Proteins were electrotransfered from the electrophoresis gel onto polyvinylidene difluoride (PVDF) membranes (Millipore, USA) at 100 V for 90 min at 4 °C. After transfer, the PVDF membranes were briefly rinsed in distilled water and incubated in Ponceau S staining solution (0.1 % [w/v] in 5 % [v/v] acetic acid) for 1 min, followed by destaining in distilled water to remove non-specific Ponceau S staining. The membranes were then inserted in between transparency sheets and imaged using a BioSpectrum® 500 imaging system (UVP). After destaining in Tris-buffered saline with Tween (TBS-T: 10 mM Tris-HCl [pH 7.4], 150 mM NaCl and 0.05 % [v/v] Tween 20), membranes were blocked with 5 % fat-free milk in TBS-T for 1 h at room temperature and then incubated with acetyl-lysine (Ac-Lys) antibody (1:1000; Cell Signaling Technology; `#9441`) at 4 °C overnight. Membranes were then washed with TBS-T and incubated for 2 h at 4 °C with alkaline phosphatase (AP)-conjugated goat anti-rabbit IgG (1:5000; Santa Cruz Biotechnology; `sc-2007`). After a final wash in TBS-T, immunoreactive proteins were detected by membrane exposure to the enhanced chemifluorescence (ECF) reagent (GE Healthcare, Piscataway, NJ, USA) followed by imaging with a BioSpectrum® 500 imaging system (UVP). Quantification by densitometric scanning (see below) was normalized to protein levels determined by Ponceau S staining (Romero-Calvo et al., 2010).

2.12 Densitometric analysis

PCR product electrophoresis, Western blot and Ponceau S staining images were quantified by densitometric scanning in ImageJ v. 1.49a (Schindelin et al., 2012).

For PCR product electrophoresis and Western blots, gels and membranes were imaged and saved as 8-bit grayscale TIFF files. Selected bands were adjusted for background noise manually using the straight line selection tool and their intensities were quantified using the gel analyzer tool. For Ponceau S staining, membranes were imaged and saved as before and adjusted for background noise using the rolling ball algorithm. Lanes were quantified using the gel analyzer tool. The linearity of Western blot and Ponceau S measurements was confirmed by including a control well with 50 % of the loaded protein – bands, lanes and regions displaying measurements within 40 % to 60 % of the respective undiluted sample were considered quantifiable. For Ac-Lys quantification, the densities of all quantifiable immunoreactive protein bands were merged.

2.13 Statistical analysis

All data are expressed as means ± SEM. The normality of distributions and the homogeneity of variances were objectively evaluated by the Shapiro–Wilk test and the F-test, respectively. Comparisons between two groups were performed using the Student t-test, the Welch t-test, the Mann–Whitney U test or Yuen's test for trimmed means, as appropriate (Wilcox, 2012). A two-sided $p < 0.05$ was considered statistically significant. All statistical analyses were performed using the R v. 3.1.2 statistical software environment (R Core Team, 2014).

Chapter 3

Results

3.1 Body, heart and liver weight

Rats were administered seven weekly injections of saline solution or DOX ($2\,\mathrm{mg\,kg^{-1}}$) and sacrificed two weeks following the last injection. All but one animal survived the entire treatment protocol. DOX-treated rats weighed significantly less than control rats at sacrifice (14 %; Table 3.1) and throughout most of the duration of the study (Fig. 3.1). No significant changes in either heart or liver weight were observed between the two treatment groups (Table 3.1). Therefore, the increase in organ:body ratios seen in DOX-treated animals reflects a change in body mass rather than alterations in organ mass (Table 3.1).

3.2 DOX alters mitochondrial biogenesis transcriptomics and mitoepigenomics

Subchronic DOX treatment alters cardiac mitochondrial function (Pereira et al., 2012). To assess if alterations to the mitochondrial biogenesis transcriptome could play a role in mitochondrial alteration, we measured transcripts of a number of genes involved in this process, including peroxisome proliferator-activated (PPAR) receptor gamma coactivator 1-alpha (PGC-1α), the master regulator of

Table 3.1
Impact of DOX treatment on body, heart and liver weights in rats

	Body weight (g)	Heart weight (g)	Liver weight (g)	Heart:body ratio ($\times 10^3$)	Liver:body ratio ($\times 10^3$)
SAL	408.0 ± 18.09	1.35 ± 0.09	13.0 ± 0.7	3.29 ± 0.17	32.0 ± 0.70
DOX	351.7 ± 6.00*	1.43 ± 0.04	13.7 ± 0.6	4.07 ± 0.11**	39.0 ± 1.65**

Heart, liver and body weights of rats treated with seven weekly injections of $2\,\mathrm{mg\,kg^{-1}}$ DOX or an equivalent volume of saline. Data are presented as means ± SEM of values from 5–6 animals in each experimental group.
*$p < 0.05$.
**$p < 0.01$.

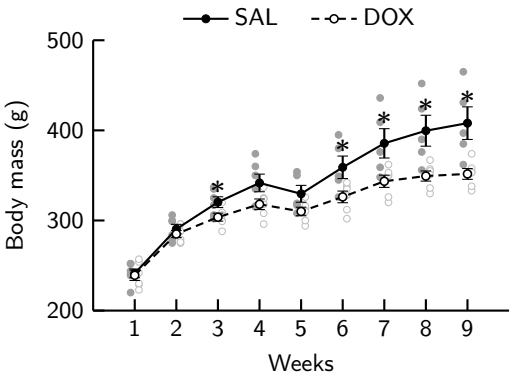

Figure 3.1. Effect of DOX treatment on body mass gain. Lines represent the means ± SEM of each experimental group at each time point. $^{*}p < 0.05$ vs. corresponding time point.

mitochondrial biogenesis, and its main downstream transcription factors (nuclear respiratory factors [NRF] -1 and -2) (Scarpulla, 2011). Subchronic DOX treatment decreased the transcript levels for *PGC-1α* (*Ppargc1a*), but did not affect *NRF-1* (*Nrf1*) and the alpha subunit of NRF-2 (*NRF-2α* [*Gabpa*]) mRNAs. In contrast, *NRF-2β* (*Gabpb1*) mRNA was significantly increased (Fig. 3.2A). Because mtDNA transcription is paramount to functional mitochondrial biogenesis, we subsequently measured the transcripts encoding for proteins that control mtDNA transcription, integrity and replication; namely mitochondrial transcription factor A (TFAM) and DNA polymerase γ (POLγ). Transcripts for *TFAM* (*Tfam*) were reduced in DOX-treated rats; however, the expression of *POLγ* (*Polg*) was unaffected (Fig. 3.2A). Increases in mitochondrial mass also involve the proliferation of mitochondrial membranes, which in turn requires de novo synthesis of cardiolipin, the main functional phospholipid of the mitochondrial inner membrane. Tafazzin (TAZ) is a transacylase required for cardiolipin metabolism that has been implicated in a number of mitochondrial disorders that culminate in cardiomyopathy (Schlame and Ren, 2006). DOX treatment induced a small, although statistically significant decrease in *TAZ* (*Taz*) mRNA levels (Fig. 3.2A).

A possible consequence of TFAM downregulation is a decrease in mtDNA quality and quantity. Indeed, in addition to its role as a mitochondrial transcription factor, TFAM is also a major component of the nucleoid – a mitochondrial maintenance structure (Campbell et al., 2012). Moreover, steady-state levels of TFAM and mtDNA display a strong correlation (Campbell et al., 2012). We therefore assessed the copy number and integrity of mtDNA – two factors that fall under the category of mitoepigenetics.* Subchronic DOX treatment significantly decreased the copy numbers of the mitochondrial *COX1* gene per nuclear $\beta_2 M$ gene in heart but not liver tissue (Fig. 3.2C), suggesting a decreased mtDNA copy number in the heart. There was no significant difference in the integrity of mtDNA extracted from heart, suggesting that there is an equal extent, if any, of mtDNA single- and double-strand break damage between both groups (Fig. 3.2B).

Finally, as a possible outcome of the above mentioned effects, we evaluated transcripts for the various components of the OxPhos machinery encoded by both the nuclear and the mitochondrial genomes. We observed a general trend towards a decrease in most of the transcripts assessed, most notably in two nDNA-encoded

*Mitoepigenetics is an umbrella term for a group of factors that affect the expression of the mitochondrial transcriptome, both nuclear and mitochondrial encoded (Ferreira et al., 2015).

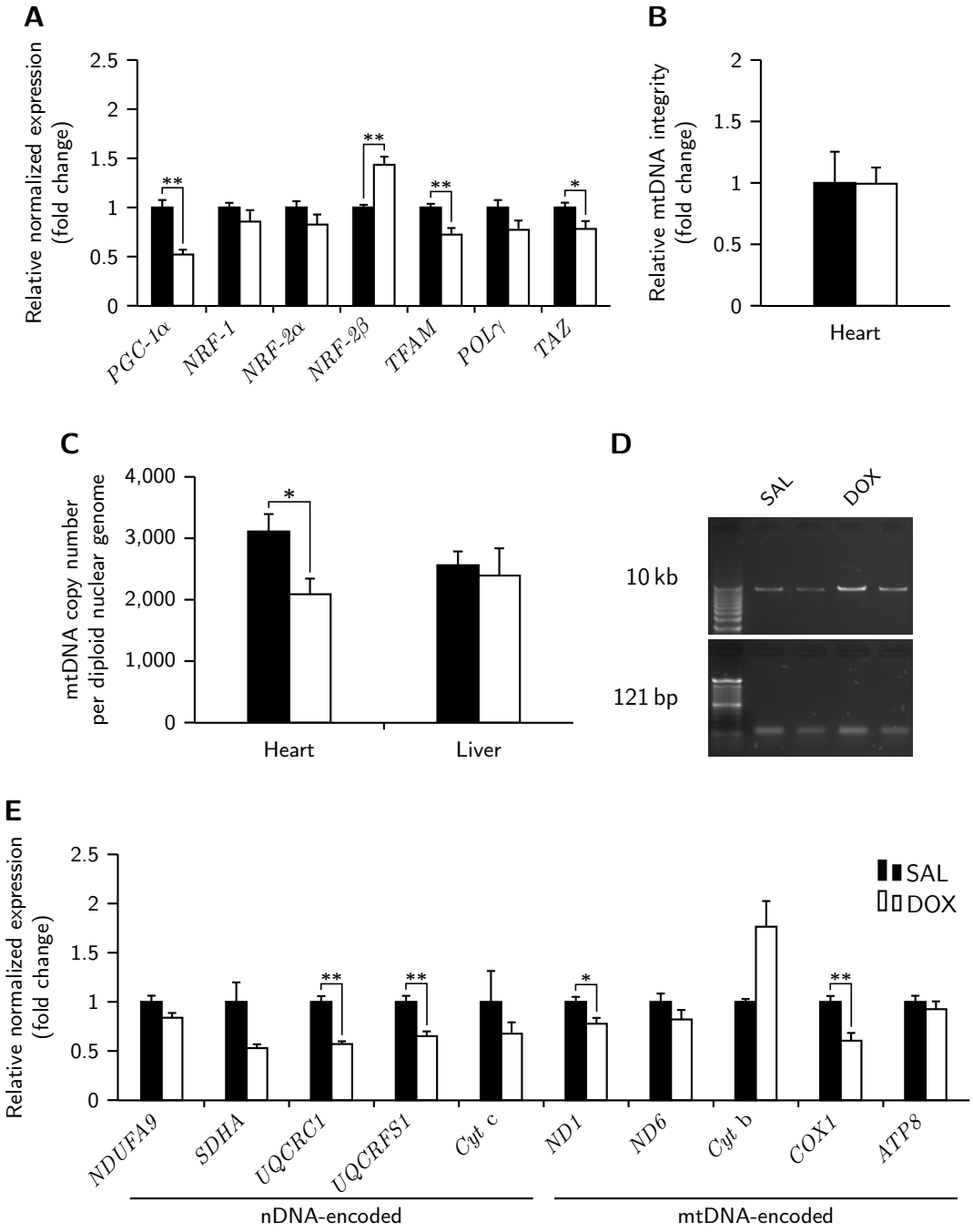

Figure 3.2. DOX compromises mitochondrial biogenesis transcriptomics and mitoepigenomics. (**A**, **E**) Heart mRNA levels of (A) proteins involved in the regulation of mitochondrial maintenance and biogenesis and (E) nuclear and mitochondrial genes encoding OxPhos subunits were quantified by qPCR and normalized to *18 S*, *TBP* and *β-actin* ($n = 4$–5 per group). (**B**) mtDNA integrity was examined by a PCR-based assay as described ($n = 5$ per group). (**C**) mtDNA copy number was measured by qPCR ($n = 3$–5 per group). (**D**) Representative gels with the 10 kb and 121 bp products. $^{*}p < 0.05$ and $^{**}p < 0.01$ for the indicated comparisons. Data are presented as means ± SEM.

complex III subunits (*UQCRC1* [*Uqcrc1*] and *UQCRFS1* [*Uqcrfs1*]), one mtDNA-encoded complex I subunit (*ND1*) and one mtDNA-encoded complex IV subunit (*COX1*). Curiously, there was a trend towards upregulation of *Cyt* b (*Mt-cyb*) mRNA, similarly observed by us in an almost identical subchronic toxicity model (Pereira et al., submitted).

3.3 DOX alters acetyl CoA metabolism and transport transcripts and changes mitochondrial protein acetylation patterns

Subchronic DOX treatment has previously been reported to decrease the expression of proteins involved in the fatty acid β-oxidation pathway (Berthiaume and Wallace, 2007b). To confirm this effect in our model, we measured the transcripts for PPARα, which regulates the transcriptional activation or repression of genes encoding for enzymes in FFA metabolism (Finck, 2007; Munday and Hemingway, 1999), as well as transcripts for enzymes involved in fatty acid β-oxidation. We observed a marked decrease in *PPARα* (*Ppara*) and for both of the assessed β-oxidation enzymes (*ACOX1* [*Acox1*], *ACAA2* [*Acaa2*]) transcripts. Interestingly, transcripts for acetyl-CoA carboxylase 2 (*ACC2* [*Acacb*]), which is repressed by PPARα (Munday and Hemingway, 1999), was also found to be reduced. Transcripts for *CACT* (*Scl25a20*), but not *ACL* (*Acly*) was also decreased, suggesting that carnitine-mediated transport of acetyl moieties between the mitochondrial and cytosolic compartments may be impaired.

To test whether these findings were relevant for protein acetylation levels and patterns, we carried out Western blot analyses of Ac-Lys in three different subcellular fractions – nuclear, mitochondrial and cytosolic –, so as to increase the spatial resolution of our findings. Total protein acetylation levels were unchanged in all of the three assessed subcellular fractions (Fig. 3.3B–D). Protein acetylation patterns, however, were found to be altered in mitochondrial fractions. SAL-treated rats displayed inconsistent levels of a ≈ 63 kDa acetylated protein band, which was found to be present in three out of five animals. In DOX-treated rats, however, this band was completely absent (Fig. 3.3C).

3.4 DOX alters the transcription and activity of histone modulators

Histone modification by HATs and HDACs is one of the major mechanisms of transcriptional regulation. The levels of these enzymes not only dictate the steady-state equilibrium of histone acetylation, but also determine the availability of these factors to be recruited to transcriptional regulatory complexes (Kouzarides, 2007). Because of their role in modulating the epigenome, we next verified whether transcripts from genes encoding HATs (*CBP* [*Crebbp*], *Ep300*, *PCAF* [*Pcaf*]) and HDACs (*HDAC1–10* [*Hdac1–10*]) were altered by DOX treatment. Two of the three HATs mRNAs assessed, *CBP* and *Ep300*, were significantly downregulated

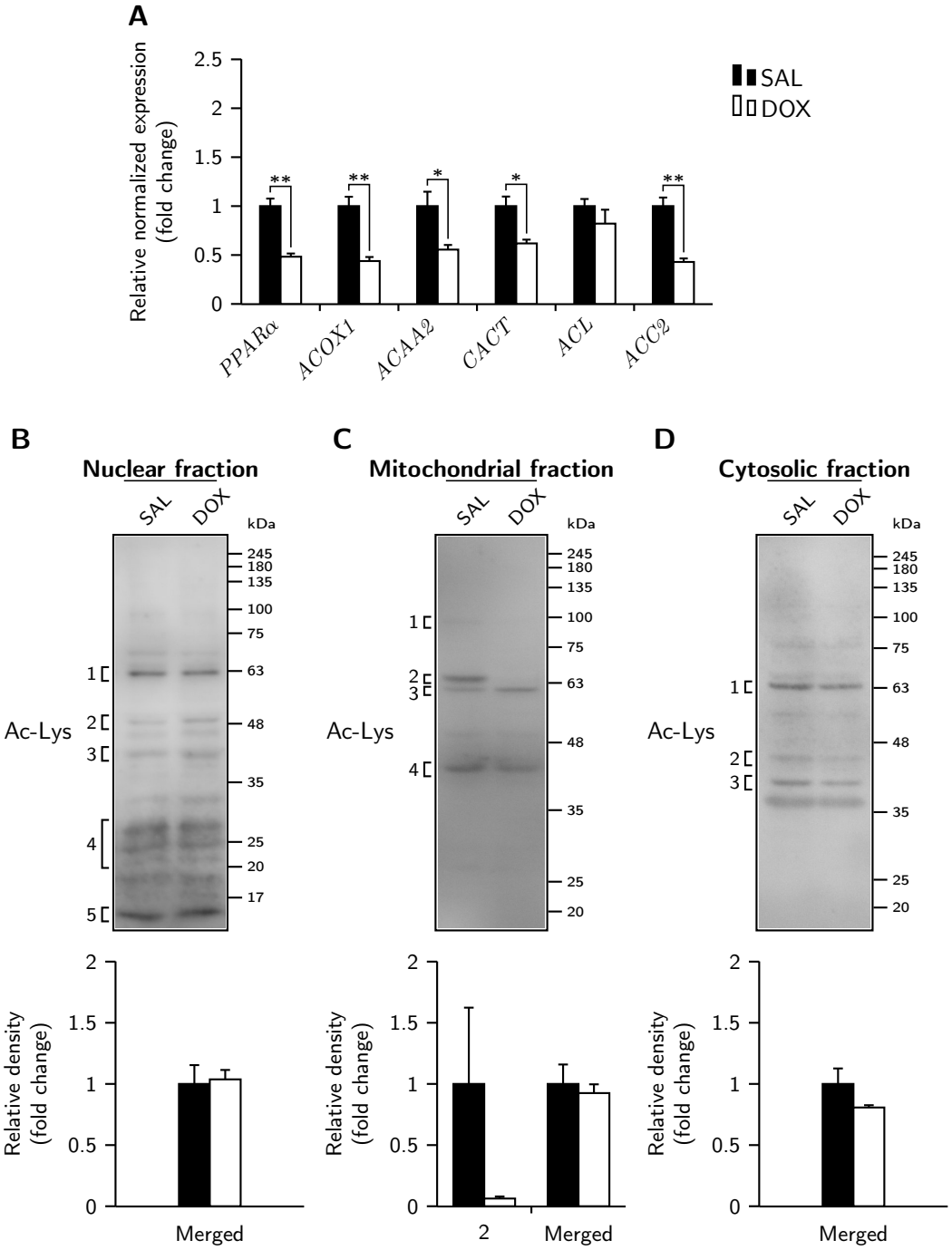

Figure 3.3. DOX alters the transcripts of genes involved in the metabolism and availability of Ac-CoA in cardiac tissue, but does not change total lysine acetylation patterns. (**A**) Heart mRNA levels of genes involved in the metabolism and transport of acetyl units were quantified by qPCR and normalized to *18 S*, *TBP* and *β-actin* ($n = 4$–5). (**B**–**D**) Representative immunoblots (top) and summarized data (bottom) of western blot experiments showing relative levels of proteins acetylated at Lys residues of (B) nuclear fractions, (C) mitochondrial fractions and (D) cytosolic fractions extracted from cardiac tissue. Numbers on the left side of blots denote regions that were deemed as quantifiable by densitometry analysis. $^{*}p < 0.05$ and $^{**}p < 0.01$ for the indicated comparisons. Data are presented as means ± SEM.

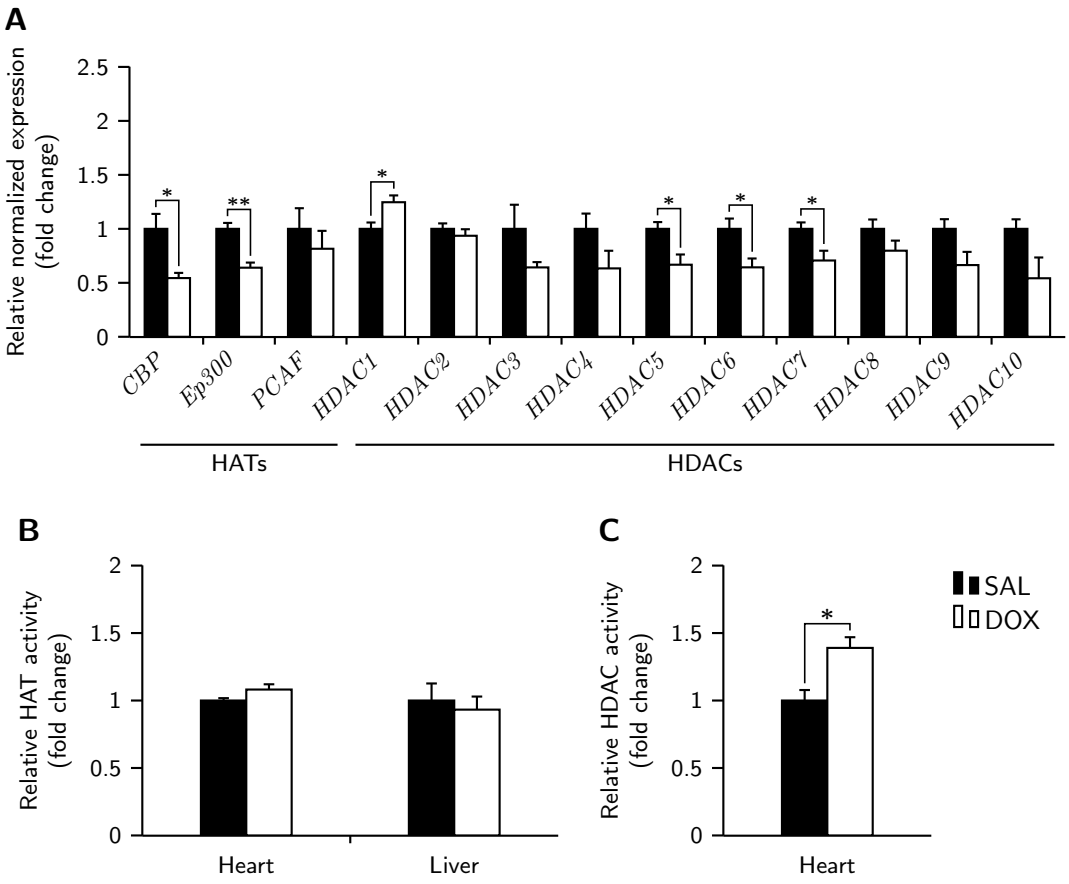

Figure 3.4. DOX alters transcripts and activity of histone modifiers. (**A**) Heart mRNA levels of genes involved in histone acetylation and deacetylation were quantified by qPCR and normalized to *18 S*, *TBP* and *β-actin* ($n = 4$–5). (**B**, **C**) The activities of (B) HATs and (C) HDACs were measured using commercial kits as described ($n = 4$–5). $^{*}p < 0.05$ and $^{**}p < 0.01$ for the indicated comparisons. Data are presented as means ± SEM.

in DOX-treated animals (Fig. 3.4A). The majority of the targeted transcripts encoding for HDACs displayed a trend towards downregulation, with a notable exception of *HDAC1* (*Hdac1*), which was found to be increased in DOX-treated animals (Fig. 3.4A).

We next investigated the activities of these two sets of enzymes. Histone acetyltransferase activity was found to be unaffected by DOX treatment in both heart and liver tissue; however, HDAC activity was increased in heart tissue (Fig. 3.4B, C).

3.5 DOX alters SAM metabolism transcripts and decreases global DNA m^5C levels in cardiac tissue

Maintenance of DNA methylation patterns is likely to depend on the levels of DNMT1 and its required substrate SAM, the synthesis of which requires the

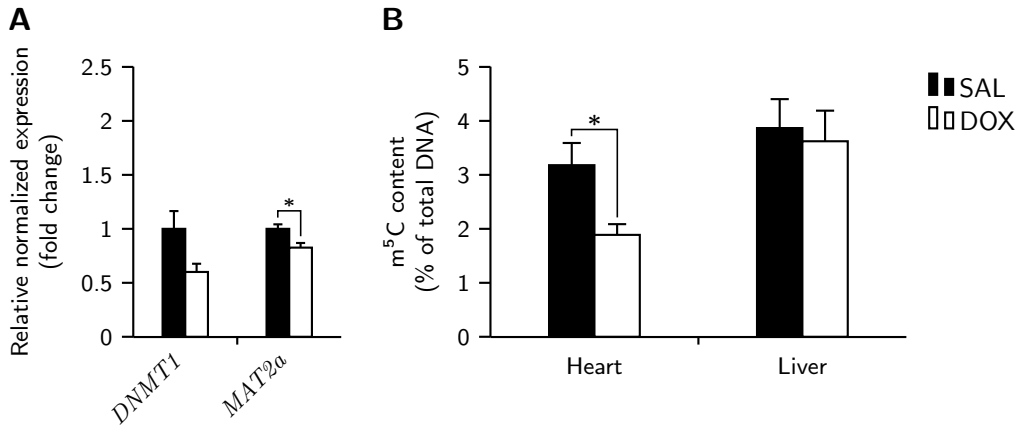

Figure 3.5. DOX decreases transcripts involved in the metabolism of SAM and decreases global m^{5}C content in cardiac tissue. (**A**) Heart mRNA levels of genes involved in DNA methylation and SAM metabolism were quantified by qPCR and normalized to *18 S*, *TBP* and *β-actin* ($n = 4$–5 per group). (**B**) Global m^{5}C content in DNA extracted from rat heart and liver tissue was examined by an ELISA assay ($n = 5$–6 per group). $^*p < 0.05$ for the indicated comparisons. Data are presented as means ± SEM.

enzyme MAT2a (Lu and Mato, 2012). Subchronic DOX treatment reduced *MAT2a* (*Mat2a*) transcripts, thus suggesting an impairment in the synthesis of SAM. However, levels of *DNMT1* (*Dnmt1*) were unaltered after DOX treatment (Fig. 3.5A).

To assess whether DOX treatment affects DNA methylation in both heart and liver tissue, total DNA extracted from both tissues was analyzed with a m^{5}C ELISA-based assay. DOX treatment resulted in a significant decrease in DNA methylation in heart but not in liver tissue (Fig. 3.5B).

Chapter 4

Discussion

Mitochondrionopathy is a well established early feature of DOX treatment (Wallace, 2003), however its role in the delayed, late-onset nature of DOX-induced cardiotoxicity remains elusive (Berthiaume and Wallace, 2007b). It is not yet clear whether the decline in cardiac metabolic function is due to compromised mitochondrial integrity and function, or rather due to a rewiring of the cardiac metabolic profile via events upstream from mitochondria. The results from our study lend credibility to our hypothesis that chronologically links both of the aforementioned events. Specifically, we propose that DOX initially disturbs the mitochondrial-dependent production of the main acetyl and methyl donors (Ac-CoA and SAM, respectively) and subsequently imprints a long lasting toxic epigenetic memory that manifests itself through an aberrant metabolic transcriptome. Herein we provide a description of the initial events relevant to out hypothesis that are taking place shortly after subchronic DOX treatment.

4.1 Mitochondrial biogenesis

As previously mentioned, disruption of mitochondrial function and biogenesis is widely acknowledged as a key component in DOX-induced cardiotoxicity (Octavia et al., 2012). Indeed, strategies aimed at increasing mitochondrial biogenesis, such as treatment with resveratrol, endurance training and stimulation of the CO/heme oxygenase (CO/HO) system, have proven to be effective in diminishing cardiac DOX toxicity (Ascensao et al., 2005; Suliman et al., 2007; Danz et al., 2009). Mitochondrial function is heavily dependent on a coordinated transcriptional regulation of both the nuclear and the mitochondrial genomes (Scarpulla, 2006). The coactivator PGC-1α has emerged as a key component in the orchestration of mitochondrial biogenesis and is highly expressed in tissues with high oxidative activity such as the heart (Ventura-Clapier et al., 2008). PGC-1α is a coactivator of the transcription factors NRF-1 and -2 that in turn promote the expression of TFAM, thus establishing a concerted activation of the nuclear and mitochondrial genomes. In the present study, we demonstrate that subchronic DOX treatment significantly decreases *PGC-1α* transcripts, as well as of its downstream target *TFAM*. Our attempts at performing western blots for these proteins were not successful; however, previous reports in the literature show that DOX decreases the

content of both PGC-1α and TFAM, albeit using different treatment protocols than our own (Suliman et al., 2007; Guo et al., 2014; Che et al., 2015). Nevertheless, decreased levels of PGC-1α and TFAM would account for the depression in nuclear- and mitochondrial-encoded OxPhos transcripts in DOX-treated rats that we observed.

Another key index of mitochondrial biogenesis, or lack thereof, is cellular mtDNA content. Our results show that DOX treatment decreases the mtDNA:nDNA copy number in cardiac tissue, which may also be implicated in the observed depression of mitochondrial-encoded OxPhos transcripts. Interestingly, we did not observe reduced mtDNA:nDNA copy numbers in liver tissue, suggesting that mtDNA alterations play a role in the cardiac-specific nature of DOX toxicity. Mitochondrial DNA strand-break damage, however, was not detected at our assessed time point. This result is not surprising, since the kinetics of the mtDNA repair machinery are likely to be able to fully cope with the rates of damage production that may be occurring at the time point we assessed. For example, in studies measuring the effect of ischemia–reperfusion in heart, known to induce an instantaneous burst of ROS (Ambrosio et al., 1991), mtDNA damage is evident after 10 min of reperfusion, but returns to baseline levels after 60 min of reperfusion (Bliksoen et al., 2015). Assuming, however, that DOX induced mtDNA strand-break damage throughout the duration of our experimental protocol, one may speculate that a possible mechanism to resolve single- and double-strand breaks would be the complete elimination of the damaged molecule, thus accounting, at least in part, for the observed depletion in mtDNA copy number. It is also important to note, however, that the assay we employed is not sensible to specific types of DNA damage that do not hamper DNA polymerase activity, such as oxidized bases. Therefore, although we have determined that subchronically DOX-treated rats do not display mtDNA strand-break lesions, mtDNA damage in the form of oxidized bases (such as 8-hydroxydeoxyguanosine [8-OHdG]) is likely to be in place, as it has already been implicated in subchronic DOX treatment (Serrano et al., 1999).

Curiously, the above results partly account for an interesting observation in a very relevant study by Lebrecht et al. (2003). The authors, employing a delayed model of subchronic DOX toxicity in Wistar rats (sacrificed 31 weeks after the last injection), demonstrated a persistent 50 % decrease in mtDNA:nDNA copy number and a selective downregulation of mitochondrial OxPhos transcripts vs. nuclear OxPhos transcripts. Consistently, they further demonstrated a selective decrease in the enzymatic activity of cytochrome *c* oxidase (COX, a multisubunit complex encoded both by nDNA and mtDNA) vs. the activity of succinate dehydrogenase (SDH, encoded entirely by nDNA), again hinting at a mitochondrial-specific transcriptional imbalance. This suggests that at later stages, the heart is able to reestablish proper nDNA-encoded mitochondrial transcript levels, but not mtDNA-encoded ones. Future studies addressing this issue should be aimed at confirming not only this observation but also additional nDNA-encoded mitochondrial transcript levels, in order to provide a definitive answer to the unilateral nuclear reestablishment of mitochondrial transcription.

4.2 Metabolism

Acetyl CoA

An additional major contributing factor to DOX-induced cardiotoxicity is the metabolic remodeling of cardiac tissue. We confirmed in our model previous results that demonstrate a decrease in transcripts involved in fatty acid oxidation in hearts from rats treated subchronically with DOX (Berthiaume and Wallace, 2007b). Importantly, this was not accompanied by an upregulation of *ACC2*, which would be expected in a programmed, well concerted metabolic shift since it encodes for an enzyme in an opposing pathway. This may be a contributing factor to the inhibition of fatty acid oxidation associated with DOX cardiotoxicity (Abdel-aleem et al., 1997; Bordoni et al., 1999).

The available literature suggests an interesting relationship between fatty acid oxidation and Ac-CoA production. There is substantial evidence implicating the carnitine shuttle system in the acquired metabolic inflexibility. For instance, Carvalho et al. (2010) showed that octanoate, a medium-chain fatty acid that does not require protein-mediated import into the mitochondrion, is equally oxidized by control and DOX treated rats. Conversely, long-chain fatty acids (which do require protein-mediated import) were shown to be inefficiently oxidized, suggesting that fatty acid transport is impaired with DOX treatment. However, no differences in gene expression or protein content of carnitine palmitoyltransferase I B (CPT1B) were found in this model (Berthiaume and Wallace, 2007b; Carvalho et al., 2010). In a study investigating the effect of L-carnitine (the cofactor of CPT1B) in fatty acid oxidation, Abdel-aleem et al. (1997) showed that the impairment in long-chain FFA oxidation is restored in DOX-treated rats co-administered L-carnitine. However, the same animals also displayed an improvement in octanoate oxidation, suggesting that L-carnitine administration may be exerting its effects on β-oxidation itself rather than on FFA transport. Indeed, taking into account that DOX greatly increases the Ac-CoA/CoA-SH ratio in isolated rat heart mitochondria (Ashour et al., 2012), it is plausible that L-carnitine acts as an Ac-CoA buffer, thus fully or partially restoring this equilibrium and thereby lifting the Ac-CoA-imposed inhibition of 3-ketoacyl-CoA thiolase – the final enzyme of the β-oxidation cycle. More importantly for our present work, however, is the possibility of maintaining normal histone acetylation dynamics by preventing the increase in Ac-CoA/CoA-SH, thus potentially ameliorating the aberrant metabolic transcriptional profile. Our results support the role of L-carnitine in buffering excess mitochondrial Ac-CoA, since the observed downregulation of *CACT* may further contribute to this metabolic instability.

Determination of the Ac-CoA/CoA-SH ratio could not be concluded at the time of this writing; however, we assessed the cellular acetylome in advance so as to posteriorly correlate this parameter with the steady-state levels of the Ac-CoA/CoA-SH pair. No differences were found in whole cell levels of acetylated proteins. However, acetylation of a ≈ 63 kDa protein was found to be absent in DOX-treated rats. Such a selective pattern of acetylation clearly indicates that in our model, whole cell protein lysine acetylation status is not limited by eventual alterations to the metabolome but is instead responding to cellular signals

that may culminate in, for example, changes in protein synthesis, degradation, translocation, repression of acetylases or activation of deacetylases.

Future work is necessary to identify the protein corresponding to the absent band. At this point in time, however, we suspect that the protein in question may be a member of the PGC-1 family for a number of reasons. First, both PGC-1α and PGC-1β are proteins subjected to dynamic acetylation and deacetylation in response to metabolic cues – particularly mediated by mitochondrial sirtuins (SIRT1, 3 and 5) (Kong et al., 2010; Canto et al., 2009; Kelly et al., 2009; Huang et al., 2010). Second, PGC-1α has been reported to colocalize in all of the three cellular compartments we assessed (nucleus, mitochondria and cytosol) (Wright et al., 2007; Safdar et al., 2011). Indeed, although PGC-1α is known to lack the canonical N-terminal mitochondrial targeting signal, it has been suggested to instead contain cryptic internal signals (Safdar et al., 2011). Third, PGC-1α is known to exist in multiple isoforms of different molecular weights in humans and mice (Ruas et al., 2012), meaning that we cannot discard the possibility of this band corresponding to PGC-1α based on its migration to a non-canonical PGC-1α molecular weight region (91–110 kDa) alone. Furthermore, the accuracy of our chosen protein marker may also be put to question. Finally, and most importantly, our failed attempts at immunoblotting PGC-1α in nuclear and mitochondrial fractions displayed the same pattern observed in close proximity to the ≈ 63 kDa region of the Ac-Lys immunoblot – that is, one single band in nuclear fractions and two bands in mitochondrial fractions (Fig. A.1). Indeed, PGC-1α is frequently reported as a double band protein in Western blot experiments (Safdar et al., 2011; Miller et al., 2012), with some authors even distinguishing between the light and heavy bands as PGC-1α and β, respectively (Garcia-Gimenez et al., 2011; Pohjoismaeki et al., 2012). Because in the PGC-1 immunoblot we did not observe the absence of the higher molecular weight band in mitochondrial fractions of DOX-treated rats, if this protein turns out to belong in fact to the PGC-1 family, then we would be confirming for the first time a selective mitochondrial deacetylation of a PGC-1 protein upon subchronic DOX treatment. We are currently working on confirming this suspicion by means of PGC-1 immunoprecipitation followed by anti Ac-Lys immunoblotting.

S-adenosyl-L-methionine

Because SAM levels are sensitive to environmental cues such as diet (Poirier et al., 2001), a strong mitochondrial toxicant such as DOX is likely to alter SAM levels as well. We are currently working on determining SAM and SAH levels by means of HPLC, but again this task is still unfinished. Nevertheless, we show that MAT2a (the enzyme that catalyzes the last step in SAM synthesis) was downregulated, suggesting that SAM synthesis may be impaired. A reduction in the SAM/SAH ratio would imply a reduction in DNA methylase activity, not only due to the limited substrate availability but also because SAH itself is a potent inhibitor of DNMTs (Selhub and Miller, 1992). Indeed, metabolic clearance of SAH is a key metabolic determinant to multiple methyltransferase reactions (Selhub and Miller, 1992). Furthermore, MAT2a has been shown to colocalize in the nucleus, specifically in chromatin-associated complexes. Absence of MAT2a

in these complexes may further compromise the local production of SAM for methyltransferases reactions (Katoh et al., 2011), which may be more meaningful than global SAM synthesis for the purposes of DNA methylation.

4.3 Epigenetics

We report for the first time that DOX treatment disturbs mRNA levels of HATs and HDACs, two important classes of histone modulators. While there were no detectable differences in HAT enzymatic activity on either heart or liver tissue, the increased activity of HDACs seen in cardiac tissue appears to correlate with the only transcript that displayed increased levels (*HDAC1*). This result suggests that the expression of HDAC proteins may be following a similar trend to the one observed in the transcription patterns. The class I HDAC family consists of HDAC1, 2, 3 and 8. These are the most significant candidates for epigenetic modulation, since they colocalize predominantly in the nucleus and possess high enzymatic activity toward histone substrates (Haberland et al., 2009). Members of the class IIa HDAC family (HDAC4, 5, 7 and 9), conversely, possess a very low catalytic activity (Fischle et al., 2002; Jones et al., 2008) and their repressive role has been attributed mostly to their function as a scaffold protein in multiprotein transcriptional repressor complexes rather than any actual catalysis (Zhang et al., 2001).* Thus, although we observe a generalized decrease in *HDAC* transcripts, our enzymatic activity assay is in agreement with a potential increased expression of class I HDAC proteins that would in turn be in concordance with the measured transcripts. To establish a correlation between this result and epigenetic modulation we intend to perform Western blot experiments against acetylated histones.

Global levels of m^5C in DNA from DOX-treated rats were found to be decreased in heart, but not liver tissue, also suggesting a relation with the cardiac-specific nature of DOX toxicity. Paradoxically, reduction in global DNA m^5C content was accompanied by a depression in the transcript levels of multiple genes. DNA methylation is an epigenetic mark mostly associated with transcriptional repression, therefore it is to be expected that a decrease in DNA methylation is followed by an increase in gene transcription. However, it is important to mention that DNA methylation is but one element in the myriad of complexity layers covering chromatin modification. In addition, the method of methylation quantification employed in this study was limited to a global analysis, and provides no information regarding gene- or region-specific differences.

Theoretically, reduced DNA methylation would be in agreement with a potential deregulation of folate metabolism and a concomitant decrease in the SAM/SAH ratio, as less methyl donors would be available to participate in DNA methylation. However, the available literature suggests that the relationship between SAM availability and DNA methylation does not follow this linear chain of thought. One in vitro study investigating the effect of folic acid supplementation in DNA

*We will leave the class IIb HDAC family (HDAC6 and 10) out of this discussion since HDAC6 is only described as a cytoplasmic cytoskeletal deacetylase (Zhang et al., 2008) and the role of HDAC10 is currently unknown (Guardiola and Yao, 2002; Haberland et al., 2009).

methylation shows that deprivation of folic acid decreases the SAM/SAH ratio but, also paradoxically, increases global DNA methylation (Farias et al., 2015). This effect appeared to be mediated mostly by changes in the expression of DNMTs 1 and 3a (which decreased by 50 % and increased by 80 %, respectively) rather than variations in the metabolome. To fully elucidate the mechanisms by which DOX decreases DNA methylation, it will be essential to measure not only SAM and SAH levels but also the protein content of the different DNA methylases.

Chapter 5

Conclusions

In summary, the present study provides new data and confirms previous data demonstrating the occurrence of metabolic and epigenetic insults as well as transcriptome disruption shortly after cessation of subchronic DOX treatment. These results are in agreement with the hypothesis that metabolite-mediated manipulation of the cardiac epigenome is an underlying factor in the persistent nature of DOX-induced cardiotoxicity. Our study provides essential substantiating evidence needed to motivate more ambitious follow-up experiments to further unravel the validity of this hypothesis using more thorough in vitro models and more expensive in vivo delayed toxicity models.

Further complementary results are needed to fully allow for the speculation of a cause and effect relationship between the initial mitochondrial injury and the also initial, albeit potentially permanent, epigenetic disruption. It will be necessary to verify if DOX-treatment disrupts the Ac-CoA/CoA-SH ratio in our experimental model and, subsequently, if the histone acetylome changes accordingly. Likewise, the SAM/SAH ratio as well as the DNA methylases protein levels will also have to be assessed in order to compare with the observed decrease in global DNA methylation. Results allowing for the establishment of the aforementioned relationship would motivate new avenues of research using primary cardiomyocytes so as to conclusively answer our experimental question. It would be interesting to verify if strategies that rescue mitochondrial function in DOX models would prevent the concurrent epigenetic and transcriptional alterations. Perhaps more interestingly, strategies using acetyl- and methyl-donor supplementation or pharmacological manipulation of epigenetic enzymes would also shed light on our question.

Appendix A

Supplementary Information

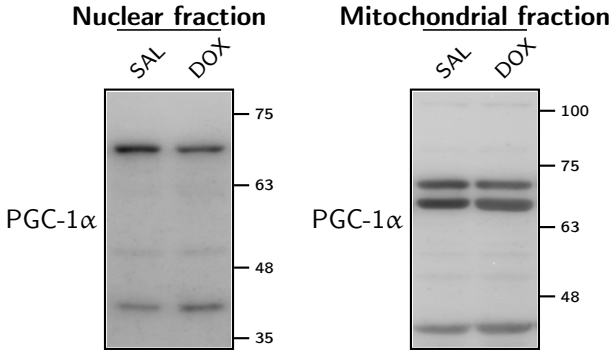

Figure A.1. Representative immunoblots of Western blot experiments showing relative levels of PGC-1α in nuclear fractions and mitochondrial fractions extracted from cardiac tissue. Western blots were carried out as described in Section 2.11 using a PGC-1 antibody (1:1000; Santa Cruz Biotechnology; `sc-13067`).

References

Abdel-aleem, S., M. M. El-Merzabani, M. Sayed-Ahmed, D. A. Taylor, and J. E. Lowe.
1997. Acute and chronic effects of adriamycin on fatty acid oxidation in isolated cardiac myocytes. *Journal of Molecular and Cellular Cardiology*, **29**(2): 789–797.
DOI: 10.1006/jmcc.1996.0323

Ambrosio, G., J. L. Zweier, and J. T. Flaherty.
1991. The relationship between oxygen radical generation and impairment of myocardial energy-metabolism following post-ischemic reperfusion. *Journal of Molecular and Cellular Cardiology*, **23**(12): 1359–1374.
DOI: 10.1016/0022-2828(91)90183-m

Arcamone, F., G. Cassinelli, G. Fantini, A. Grein, P. Orezzi, C. Pol, and C. Spalla.
1969. Adriamycin, 14-hydroxydaunomycin, a new antitumor antibiotic from *S. peucetius* var. *caesius*. *Biotechnology and Bioengineering*, **11**(6): 1101–1110.
DOI: 10.1002/bit.260110607

Ascensao, A., J. Magalhaes, J. M. C. Soares, R. Ferreira, M. J. Neuparth, F. Marques, P. J. Oliveira, and J. A. Duarte.
2005. Moderate endurance training prevents doxorubicin-induced in vivo mitochondriopathy and reduces the development of cardiac apoptosis. *American Journal of Physiology-Heart and Circulatory Physiology*, **289**(2): H722–H731.
DOI: 10.1152/ajpheart.01249.2004

Ascensao, A., R. Ferreira, P. J. Oliveira, and J. Magalhaes.
2006. Effects of endurance training and acute doxorubicin treatment on rat heart mitochondrial alterations induced by in vitro anoxia-reoxygenation. *Cardiovascular Toxicology*, **6**(3–4): 159–171.
DOI: 10.1385/ct:6:3:159

Ashour, A. E., M. M. Sayed-Ahmed, A. R. Abd-Allah, H. M. Korashy, Z. H. Maayah, H. Alkhalidi, M. Mubarak, and A. Alhaider.
2012. Metformin rescues the myocardium from doxorubicin-induced energy starvation and mitochondrial damage in rats. *Oxidative Medicine and Cellular Longevity*.
DOI: 10.1155/2012/434195

Aversano, R. C. and P. J. Boor.
1983. Histochemical alterations of acute and chronic doxorubicin cardiotoxicity. *Journal of Molecular and Cellular Cardiology*, **15**(8): 543–553.
DOI: 10.1016/0022-2828(83)90330-9

Aykin-Burns, N., I. M. Ahmad, Y. Zhu, L. W. Oberley, and D. R. Spitz.
2009. Increased levels of superoxide and H_2O_2 mediate the differential susceptibility of cancer cells versus normal cells to glucose deprivation. *Biochemical Journal*, **418**: 29–37.
DOI: 10.1042/bj20081258

Bachur, N. R., S. L. Gordon, and M. V. Gee.
1977. Anthracycline antibiotic augmentation of microsomal electron transport and free radical formation. *Molecular Pharmacology*, **13**(5): 901–910.

Bachur, N. R., M. V. Gee, and R. D. Friedman.
1982. Nuclear catalyzed antibiotic free radical formation. *Cancer Research*, **42**(3): 1078–1081.

Bannister, A. J. and T. Kouzarides.
2011. Regulation of chromatin by histone modifications. *Cell Research*, **21**(3): 381–395.
DOI: 10.1038/cr.2011.22

Barth, E., G. Stammler, B. Speiser, and J. Schaper.
1992. Ultrastructural Quantitation of Mitochondria and Myofilaments in Cardiac Muscle From 10 Different Animal Species Including Man. *Journal of Molecular and Cellular Cardiology*, **24**(7): 669–681.
DOI: 10.1016/0022-2828(92)93381-s

Benson, D. A., K. Clark, I. Karsch-Mizrachi, D. J. Lipman, J. Ostell, and E. W. Sayers.
2014. GenBank. *Nucleic Acids Research*, **42**(D1): D32–D37.
DOI: 10.1093/nar/gkt1030

Beretta, G. L. and F. Zunino.
2008. "Molecular Mechanisms of Anthracycline Activity". *Anthracycline Chemistry and Biology II*. Ed. by K. Krohn. Springer Berlin Heidelberg.
DOI: 10.1007/128_2007_3

Berger, S. L., T. Kouzarides, R. Shiekhattar, and A. Shilatifard.
2009. An operational definition of epigenetics. *Genes & Development*, **23**(7): 781–783.
DOI: 10.1101/gad.1787609

Berthiaume, J. M. and K. B. Wallace.
2007a. Adriamycin-induced oxidative mitochondrial cardiotoxicity. *Cell Biology and Toxicology*, **23**(1): 15–25.
DOI: 10.1007/s10565-006-0140-y

Berthiaume, J. M. and K. B. Wallace.
2007b. Persistent Alterations to the Gene Expression Profile of the Heart Subsequent to Chronic Doxorubicin Treatment. *Cardiovascular Toxicology*, **7**(3): 178–191.
DOI: 10.1007/s12012-007-0026-0

Bird, A. P. and A. P. Wolffe.
1999. Methylation-Induced Repression – Belts, Braces, and Chromatin. *Cell*, **99**(5): 451–454.
DOI: 10.1016/s0092-8674(00)81532-9

Bliksoen, M., A. Baysa, L. Eide, M. Bjoras, R. Suganthan, J. Vaage, K. O. Stenslokken, and G. Valen.
2015. Mitochondrial DNA damage and repair during ischemia-reperfusion injury of the heart. *Journal of Molecular and Cellular Cardiology*, **78**: 9–22.
DOI: 10.1016/j.yjmcc.2014.11.010

Bordoni, A., P. L. Biagi, and S. Hrelia.
1999. The impairment of essential fatty acid metabolism as a key factor in doxorubicin-induced damage in cultured rat cardiomyocytes. *Biochimica Et Biophysica Acta-Molecular and Cell Biology of Lipids*, **1440**(1): 100–106.
DOI: 10.1016/s1388-1981(99)00113-4

Box, V. G.
2007. The intercalation of DNA double helices with doxorubicin and nagalomycin. *Journal of Molecular Graphics and Modelling*, **26**(1): 14–19.
DOI: 10.1016/j.jmgm.2006.09.005

Bremer, J.
1983. Carnitine – Metabolism and Functions. *Physiological Reviews*, **63**(4): 1420–1480.

Bremerskov, V. and R. Linnemann.
1969. Some Effects of Daunomycin on the Nucleic Acid Synthesis in Sychronized *L*-Cells. *European Journal of Cancer*, **5**(4): 317–330.
DOI: 10.1016/0014-2964(69)90045-0

Calendi, E., A. Di Marco, M. Reggiani, B. Scarpinato, and L. Valentini.
1965. On physico-chemical interactions between daunomycin and nucleic acids. *Biochimica et Biophysica Acta*, **103**(1): 25–49.
DOI: 10.1016/0005-2787(65)90539-3

Campbell, C. T., J. E. Kolesar, and B. A. Kaufman.
2012. Mitochondrial transcription factor A regulates mitochondrial transcription initiation, DNA packaging, and genome copy number. *Biochimica et Biophysica Acta (BBA) - Gene Regulatory Mechanisms*, **1819**(9-10): 921–929.
DOI: 10.1016/j.bbagrm.2012.03.002

Canto, C., Z. Gerhart-Hines, J. N. Feige, M. Lagouge, L. Noriega, J. C. Milne, P. J. Elliott, P. Puigserver, and J. Auwerx.
2009. AMPK regulates energy expenditure by modulating NAD^+ metabolism and SIRT1 activity. *Nature*, **458**(7241): 1056–U140.
DOI: 10.1038/nature07813

Carvalho, C., R. X. Santos, S. Cardoso, S. Correia, P. J. Oliveira, M. S. Santos, and P. I. Moreira.
2009. Doxorubicin: The Good, the Bad and the Ugly Effect. *Current Medicinal Chemistry*, **16**(25): 3267–3285.
DOI: 10.2174/092986709788803312

Carvalho, R. A., R. P. B. Sousa, V. J. J. Cadete, G. D. Lopaschuk, C. M. M. Palmeira, J. A. Bjork, and K. B. Wallace.
2010. Metabolic remodeling associated with subchronic doxorubicin cardiomyopathy. *Toxicology*, **270**(2-3): 92–98.
DOI: 10.1016/j.tox.2010.01.019

Champoux, J. J.
2001. DNA topoisomerases: Structure, function, and mechanism. *Annual Review of Biochemistry*, **70**: 369–413.
DOI: 10.1146/annurev.biochem.70.1.369

Chandran, K., D. Aggarwal, R. Q. Migrino, J. Joseph, D. McAllister, E. A. Konorev, W. E. Antholine, J. Zielonka, S. Srinivasan, N. G. Avadhani, and B. Kalyanaraman.
2009. Doxorubicin Inactivates Myocardial Cytochrome *c* Oxidase in Rats: Cardioprotection by Mito-Q. *Biophysical Journal*, **96**(4): 1388–1398.
DOI: 10.1016/j.bpj.2008.10.042

Che, R., C. Zhu, G. Ding, M. Zhao, M. Bai, Z. Jia, A. Zhang, and S. Huang.
2015. Huaier cream protects against adriamycin-induced nephropathy by restoring mitochondrial function via PGC-1α upregulation. *Ppar Research*.
DOI: 10.1155/2015/720383

Chestnut, B. A., Q. Chang, A. Price, C. Lesuisse, M. Wong, and L. J. Martin.
2011. Epigenetic Regulation of Motor Neuron Cell Death through DNA Methylation. *Journal of Neuroscience*, **31**(46): 16619–16636.
DOI: 10.1523/jneurosci.1639-11.2011

Childs, A. C., S. L. Phaneuf, A. J. Dirks, T. Phillips, and C. Leeuwenburgh.
2002. Doxorubicin treatment in vivo causes cytochrome *c* release and cardiomyocyte apoptosis, as well as increased mitochondrial efficiency, superoxide dismutase activity, and Bcl-2:Bax ratio. *Cancer Research*, **62**(16): 4592–4598.

Chu, C. H., L. F. Mao, and H. Schulz.
1994. Estimation of peroxisomal β-oxidation in rat heart by a direct assay of acyl-CoA oxidase. *Biochemical Journal*, **302**: 23–29.

Coldwell, K. E., S. M. Cutts, T. J. Ognibene, P. T. Henderson, and D. R. Phillips.
2008. Detection of Adriamycin-DNA adducts by accelerator mass spectrometry at clinically relevant Adriamycin concentrations. *Nucleic Acids Research*, **36**(16): e100.
DOI: 10.1093/nar/gkn439

Collins, L. J., B. Schonfeld, and X. S. Chen.
2011. "The Epigenetics of Non-coding RNA". *Handbook of Epigenetics*. Ed. by T. Tollefsbol. Elsevier.
DOI: http://dx.doi.org/10.1016/B978-0-12-375709-8.00004-6

Crowell, A. M. J., M. J. Wall, and A. A. Doucette.
2013. Maximizing recovery of water-soluble proteins through acetone precipitation. *Analytica*

Chimica Acta, **796**: 48–54.
DOI: 10.1016/j.aca.2013.08.005

Cui, X.-S., D.-X. Zhang, Y.-G. Ko, and N.-H. Kim.
2009. Aberrant epigenetic reprogramming of imprinted *microRNA-127* and *Rtl1* in cloned mouse embryos. *Biochemical and Biophysical Research Communications*, **379**(2): 390–394.
DOI: 10.1016/j.bbrc.2008.12.148

Danz, E. D. B., J. Skramsted, N. Henry, J. A. Bennett, and R. S. Keller.
2009. Resveratrol prevents doxorubicin cardiotoxicity through mitochondrial stabilization and the Sirt1 pathway. *Free Radical Biology and Medicine*, **46**(12): 1589–1597.
DOI: 10.1016/j.freeradbiomed.2009.03.011

Davies, K. J. A. and J. H. Doroshow.
1986. Redox Cycling of Anthracyclines by Cardiac Mitochondria. *Journal of Biological Chemistry*, **261**(7): 3060–3067.

Depeint, F., W. R. Bruce, N. Shangari, R. Mehta, and P. J. O'Brien.
2006. Mitochondrial function and toxicity: Role of B vitamins on the one-carbon transfer pathways. *Chemico-Biological Interactions*, **163**(1–2): 113–132.
DOI: 10.1016/j.cbi.2006.05.010

Di Marco, A., R. Silvestrini, S. Di Marco, and T. Dasdia.
1965. Inhibiting effect of new cytotoxic antibiotic daunomycin on nucleic acids and mitotic activity of HeLa cells. *Journal of Cell Biology*, **27**(3): 545–550.
DOI: 10.1083/jcb.27.3.545

Dimauro, I., T. Pearson, D. Caporossi, and M. J. Jackson.
2012. A simple protocol for the subcellular fractionation of skeletal muscle cells and tissue. *BMC research notes*, **5**: 513–513.
DOI: 10.1186/1756-0500-5-513

Doroshow, J. H., G. Y. Locker, and C. E. Myers.
1980. Enzymatic Defenses of the Mouse Heart Against Reactive Oxygen Metabolites – Alterations Produced by Doxorubicin. *Journal of Clinical Investigation*, **65**(1): 128–135.
DOI: 10.1172/jci109642

Farias, N., N. Ho, S. Butler, L. Delaney, J. Morrison, S. Shahrzad, and B. L. Coomber.
2015. The effects of folic acid on global DNA methylation and colonosphere formation in colon cancer cell lines. *The Journal of nutritional biochemistry*, **26**(8): 818–26.
DOI: 10.1016/j.jnutbio.2015.02.002

Ferreira, A., T. L. Serafim, V. A. Sardao, and T. Cunha-Oliveira.
2015. Role of mtDNA-related mitoepigenetic phenomena in cancer. *European Journal of Clinical Investigation*, **45**: 44–49.
DOI: 10.1111/eci.12359

Finck, B. N.
2007. The PPAR regulatory system in cardiac physiology and disease. *Cardiovascular Research*, **73**(2): 269–277.
DOI: 10.1016/j.cardiores.2006.08.023

Fischle, W., F. Dequiedt, M. J. Hendzel, M. G. Guenther, M. A. Lazar, W. Voelter, and E. Verdin.
2002. Enzymatic activity associated with class II HDACs is dependent on a multiprotein complex containing HDAC3 and SMRT/N-CoR. *Molecular Cell*, **9**(1): 45–57.
DOI: 10.1016/s1097-2765(01)00429-4

Flint, D. H., J. F. Tuminello, and M. H. Emptage.
1993. The Inactivation of Fe−S Cluster Containing Hydro-lyases by Superoxide. *Journal of Biological Chemistry*, **268**(30): 22369–22376.

Fox, J. T. and P. J. Stover.
2008. Folate-Mediated One-Carbon Metabolism. *Folic Acid and Folates*, **79**: 1–44.
DOI: 10.1016/s0083-6729(08)00401-9

Friedman, M. A., M. J. Bozdech, M. E. Billingham, and A. K. Rider.
1978. Doxorubicin Cardiotoxicity – Serial Endomyocardial Biopsies and Systolic Time

Intervals. *Journal of the American Medical Association*, **240**(15): 1603–1606.
DOI: 10.1001/jama.240.15.1603

Garcia-Gimenez, J. L., A. Gimeno, P. Gonzalez-Cabo, F. Dasi, A. Bolinches-Amoros, B. Molla, F. Palau, and F. V. Pallardo.
2011. Differential expression of PGC-1α and metabolic sensors suggest age-dependent induction of mitochondrial biogenesis in Friedreich ataxia fibroblasts. *Plos One*, **6**(6).
DOI: 10.1371/journal.pone.0020666

Gewirtz, D. A.
1999. A Critical Evaluation of the Mechanisms of Action Proposed for the Antitumor Effects of the Anthracycline Antibiotics Adriamycin and Daunorubicin. *Biochemical Pharmacology*, **57**(7): 727–741.
DOI: 10.1016/s0006-2952(98)00307-4

Goormaghtigh, E., P. Chatelain, J. Caspers, and J. M. Ruysschaert.
1980. Evidence of a complex between adriamycin derivatives and cardiolipin: Possible role in cardiotoxicity. *Biochemical Pharmacology*, **29**(21): 3003–3010.
DOI: 10.1016/0006-2952(80)90050-7

Guardiola, A. R. and T. P. Yao.
2002. Molecular cloning and characterization of a novel histone deacetylase HDAC10. *Journal of Biological Chemistry*, **277**(5): 3350–3356.
DOI: 10.1074/jbc.M109861200

Guibert, S. and M. Weber.
2013. Functions of DNA Methylation and Hydroxymethylation in Mammalian Development. *Epigenetics and Development*, **104**: 47–83.
DOI: 10.1016/b978-0-12-416027-9.00002-4

Guo, J., Q. Guo, H. Fang, L. Lei, T. Zhang, J. Zhao, and S. Peng.
2014. Cardioprotection against doxorubicin by metallothionein Is associated with preservation of mitochondrial biogenesis involving PGC-1α pathway. *European Journal of Pharmacology*, **737**: 117–124.
DOI: 10.1016/j.ejphar.2014.05.017

Haberland, M., R. L. Montgomery, and E. N. Olson.
2009. The many roles of histone deacetylases in development and physiology: implications for disease and therapy. *Nature Reviews Genetics*, **10**(1): 32–42.
DOI: 10.1038/nrg2485

Halliwell, B. and C. E. Cross.
1994. Oxygen-derived Species: Their Relation to Human Disease and Environmental Stress. *Environmental Health Perspectives*, **102**: 5–12.
DOI: 10.2307/3432205

Huang, J.-Y., M. D. Hirschey, T. Shimazu, L. Ho, and E. Verdin.
2010. Mitochondrial sirtuins. *Biochimica Et Biophysica Acta-Proteins and Proteomics*, **1804**(8): 1645–1651.
DOI: 10.1016/j.bbapap.2009.12.021

Iacobazzi, V., A. Castegna, V. Infantino, and G. Andria.
2013. Mitochondrial DNA methylation as a next-generation biomarker and diagnostic tool. *Molecular Genetics and Metabolism*, **110**(1–2): 25–34.
DOI: 10.1016/j.ymgme.2013.07.012

Idell-Wenger, J. A., L. W. Grotyohann, and J. R. Neely.
1978. Coenzyme A and Carnitine Distribution in Normal and Ischemic Hearts. *Journal of Biological Chemistry*, **253**(12): 4310–4318.

Jeltsch, A.
2006. On the Enzymatic Properties of Dnmt1: Specificity, Processivity, Mechanism of Linear Diffusion and Allosteric Regulation of the Enzyme. *Epigenetics*, **1**(2): 63–66.
DOI: 10.4161/epi.1.2.2767

Ji, L. L. and E. W. Mitchell.
1994. Effects of adriamycin on heart mitochondrial funtion in rested and exercised rats. *Biochemical Pharmacology*, **47**(5): 877–885.

Jones, P., S. Altamura, A. De Francesco, P. Gallinari, A. Lahm, P. Neddermann, M. Rowley, S. Serafini, and C. Steinkuehler.
2008. Probing the elusive catalytic activity of vertebrate class IIa histone deacetylases. *Bioorganic & Medicinal Chemistry Letters*, **18**(6): 1814–1819.
DOI: 10.1016/j.bmcl.2008.02.025

Katoh, Y., T. Ikura, Y. Hoshikawa, S. Tashiro, T. Ito, M. Ohta, Y. Kera, T. Noda, and K. Igarashi.
2011. Methionine adenosyltransferase II serves as a transcriptional corepressor of Maf oncoprotein. *Molecular Cell*, **41**(5): 554–566.
DOI: 10.1016/j.molcel.2011.02.018

Kelly, T. J., C. Lerin, W. Haas, S. P. Gygi, and P. Puigserver.
2009. GCN5-mediated transcriptional control of the metabolic coactivator PGC-1β through lysine acetylation. *Journal of Biological Chemistry*, **284**(30): 19945–19952.
DOI: 10.1074/jbc.M109.015164

Kong, X., R. Wang, Y. Xue, X. Liu, H. Zhang, Y. Chen, F. Fang, and Y. Chang.
2010. Sirtuin 3, a new target of PGC-1α, plays an important role in the suppression of ROS and mitochondrial biogenesis. *Plos One*, **5**(7): Jul.
DOI: 10.1371/journal.pone.0011707

Kouzarides, T.
2007. Chromatin modifications and their function. *Cell*, **128**(4): 693–705.
DOI: 10.1016/j.cell.2007.02.005

Kovalenko, O. A. and J. H. Santos.
2009. Analysis of oxidative damage by gene-specific quantitative PCR. *Current protocols in human genetics*, **19**: 19.1.1–19.1.13.
DOI: 10.1002/0471142905.hg1901s62

Krohn, K.
2008. *Anthracycline Chemistry and Biology II: Mode of Action, Clinical Aspects and New Drugs*. Springer.
DOI: 10.1007/978-3-540-75813-6

Laatsch, H. and S. Fotso.
2008. "Naturally Occurring Anthracyclines". *Anthracycline Chemistry and Biology I: Biological Occurence and Biosynthesis, Synthesis and Chemistry*. Ed. by K. Krohn. Springer Berlin Heidelberg.
DOI: 10.1007/128_2008_5

Larsen, A. K., A. E. Eseargueil, and A. Skladanowski.
2003. Catalytic topoisomerase II inhibitors in cancer therapy. *Pharmacology & Therapeutics*, **99**(2): 167–181.
DOI: 10.1016/s0163-7258(03)00058-5

Lebrecht, D., B. Setzer, U. P. Ketelsen, J. Haberstroh, and U. A. Walker.
2003. Time-dependent and tissue-specific accumulation of mtDNA and respiratory chain defects in chronic doxorubicin cardiomyopathy. *Circulation*, **108**(19): 2423–2429.
DOI: 10.1161/01.cir.00000931963.59829.df

Lebrecht, D., A. Kokkori, U.-P. Ketelsen, B. Setzer, and U. A. Walker.
2005. Tissue-specific mtDNA lesions and radical-associated mitochondrial dysfunction in human hearts exposed to doxorubicin. *The Journal of Pathology*, **207**(4): 436–444.
DOI: 10.1002/path.1863

Lefrak, E. A., J. Pitha, Rosenhei.S, and J. A. Gottlieb.
1973. A clinicopathologic analysis of adriamycin cardiotoxicity. *Cancer*, **32**(2): 302–314.
DOI: 10.1002/1097-0142(197308)32:2<302::aid-cncr2820320205>3.0.co;2-2

Lu, C. and C. B. Thompson.
2012. Metabolic Regulation of Epigenetics. *Cell Metabolism*, **16**(1): 9–17.
DOI: 10.1016/j.cmet.2012.06.001

Lu, S. C.
2009. Regulation of glutathione synthesis. *Molecular Aspects of Medicine*, **30**(1-2): 42–59.
DOI: 10.1016/j.mam.2008.05.005

Lu, S. C. and J. M. Mato.
2012. *S*-adenosylmethionine in liver health, injury, and cancer. *Physiological Reviews*, **92**(4): 1515–1542.
DOI: 10.1152/physrev.00047.2011

Luger, K. and J. C. Hansen.
2005. Nucleosome and chromatin fiber dynamics. *Current Opinion in Structural Biology*, **15**(2): 188–196.
DOI: 10.1016/j.sbi.2005.03.006

Madiraju, P., S. V. Pande, M. Prentki, and S. R. M. Madiraju.
2009. Mitochondrial acetylcarnitine provides acetyl groups for nuclear histone acetylation. *Epigenetics*, **4**(6): 296–299.

Miller, B. F., M. M. Robinson, M. D. Bruss, M. Hellerstein, and K. L. Hamilton.
2012. A comprehensive assessment of mitochondrial protein synthesis and cellular proliferation with age and caloric restriction. *Aging Cell*, **11**(1): 150–161.
DOI: 10.1111/j.1474-9726.2011.00769.x

Mimnaugh, E. G., M. A. Trush, M. Bhatnagar, and T. E. Gram.
1985. Enhancement of reactive oxygen-dependent mitochondrial membrane lipid peroxidation by the anticancer drug adriamycin. *Biochemical Pharmacology*, **34**(6): 847–856.
DOI: 10.1016/0006-2952(85)90766-x

Montaigne, D., X. Marechal, R. Baccouch, T. Modine, S. Preau, K. Zannis, P. Marchetti, S. Lancel, and R. Neviere.
2010. Stabilization of mitochondrial membrane potential prevents doxorubicin-induced cardiotoxicity in isolated rat heart. *Toxicology and Applied Pharmacology*, **244**(3): 300–307.
DOI: 10.1016/j.taap.2010.01.006

Munday, M. R. and C. J. Hemingway.
1999. The regulation of acetyl-CoA carboxylase – A potential target for the action of hypolipidemic agents. *Advances in Enzyme Regulation*, **39**: 205–234.
DOI: 10.1016/s0065-2571(98)00016-8

Naviaux, R. K.
2008. Mitochondrial control of epigenetics. *Cancer Biology & Therapy*, **8**(7): 1191–1193.

Nicolay, K., J. J. Fok, W. Voorhout, J. A. Post, and B. Dekruijff.
1986. Cytofluorescence detection of adriamycin-mitochondria interactions in isolated, perfused rat heart. *Biochimica Et Biophysica Acta*, **887**(1): 35–41.
DOI: 10.1016/0167-4889(86)90119-9

Nitiss, J. L.
1998. Investigating the biological functions of DNA topoisomerases in eukaryotic cells. *Biochimica Et Biophysica Acta-Gene Structure and Expression*, **1400**(1–3): 63–81.
DOI: 10.1016/s0167-4781(98)00128-6

Nunn, C. M., L. Vanmeervelt, S. Zhang, M. H. Moore, and O. Kennard.
1991. DNA-Drug Interactions – The Crystal Structures of d(TGTACA) and d(TGATCA) Complexed with Daunomycin. *Journal of Molecular Biology*, **222**(2): 167–177.
DOI: 10.1016/0022-2836(91)90203-i

Octavia, Y., C. G. Tocchetti, K. L. Gabrielson, S. Janssens, H. J. Crijns, and A. L. Moens.
2012. Doxorubicin-induced cardiomyopathy: From molecular mechanisms to therapeutic strategies. *Journal of Molecular and Cellular Cardiology*, **52**(6): 1213–1225.
DOI: 10.1016/j.yjmcc.2012.03.006

Okano, M., S. P. Xie, and E. Li.
1998. Cloning and characterization of a family of novel mammalian DNA (cytosine-5)

methyltransferases. *Nature Genetics*, **19**(3): 219–220.
DOI: 10.1038/890

Okano, M., D. W. Bell, D. A. Haber, and E. Li.
1999. DNA methyltransferases Dnmt3a and Dnmt3b are essential for de novo methylation and mammalian development. *Cell*, **99**(3): 247–257.
DOI: 10.1016/s0092-8674(00)81656-6

Oliveira, P. J., J. A. Bjork, M. S. Santos, R. L. Leino, M. K. Froberg, A. J. Moreno, and K. B. Wallace.
2004. Carvedilol-mediated antioxidant protection against doxorubicin-induced cardiac mitochondrial toxicity. *Toxicology and Applied Pharmacology*, **200**(2): 159–168.
DOI: 10.1016/j.taap.2004.04.005

Oram, J. F., S. L. Bennetch, and J. R. Neely.
1973. Regulation of Fatty Acid Utilization in Isolated Perfused Hearts. *Journal of Biological Chemistry*, **248**(15): 5299–5309.

Oram, J. F., J. I. Wenger, and J. R. Neely.
1975. Regulation of Long Chain Fatty Acid Activation in Heart Muscle. *Journal of Biological Chemistry*, **250**(1): 73–78.

Ott, M., J. D. Robertson, V. Gogvadze, B. Zhivotovsky, and S. Orrenius.
2002. Cytochrome *c* release from mitochondria proceeds by a two-step process. *Proceedings of the National Academy of Sciences of the United States of America*, **99**(3): 1259–1263.
DOI: 10.1073/pnas.241655498

Ozdemir, A., H. Masumoto, P. Fitzjohn, A. Verreault, and C. Logie.
2006. Histone H3 Lysine 56 Acetylation – A New Twist in the Chromosome Cycle. *Cell Cycle*, **5**(22): 2602–2608.
DOI: 10.4161/cc.5.22.3473

Palmeira, C. M., J. Serrano, D. W. Kuehl, and K. B. Wallace.
1997. Preferential oxidation of cardiac mitochondrial DNA following acute intoxication with doxorubicin. *Biochimica et Biophysica Acta-Bioenergetics*, **1321**(2): 101–106.
DOI: 10.1016/s0005-2728(97)00055-8

Pereira, G. C., S. P. Pereira, C. V. Pereira, J. A. Lumini, J. Magalhaes, A. Ascensao, M. S. Santos, A. J. Moreno, and P. J. Oliveira.
2012. Mitochondrionopathy phenotype in doxorubicin-treated Wistar rats depends on treatment protocol and is cardiac-specific. *PLoS ONE*, **7**(6): e38867.
DOI: 10.1371/journal.pone.0038867

Peters, J. H., G. R. Gordon, D. Kashiwase, and E. M. Acton.
1981. Tissue Distribution of Doxorubicin and Doxorubicinol in Rats Receiving Multiple Doses of Doxorubicin. *Cancer Chemotherapy and Pharmacology*, **7**(1): 65–69.

Pfaffl, M. W.
2001. A new mathematical model for relative quantification in real-time RT-PCR. *Nucleic Acids Research*, **29**(9).
DOI: 10.1093/nar/29.9.e45

Pirrotta, V.
1999. Transvection and chromosomal *trans*-interaction effects. *Biochimica Et Biophysica Acta-Reviews on Cancer*, **1424**(1): M1–M8.
DOI: 10.1016/S0304-419X(99)00019-0

Pohjoismaeki, J. L. O., T. Boettger, Z. Liu, S. Goffart, M. Szibor, and T. Braun.
2012. Oxidative stress during mitochondrial biogenesis compromises mtDNA integrity in growing hearts and induces a global DNA repair response. *Nucleic Acids Research*, **40**(14): 6595–6607.
DOI: 10.1093/nar/gks301

Poirier, L. A., C. K. Wise, R. R. Delongchamp, and R. Sinha.
2001. Blood determinations of *S*-adenosylmethionine, *S*-adenosylhomocysteine, and homocysteine: Correlations with diet. *Cancer Epidemiology Biomarkers & Prevention*, **10**(6): 649–655.

Quigley, G. J., A. H. J. Wang, G. Ughetto, G. Vandermarel, J. H. Vanboom, and A. Rich.
1980. Molecular structure of an anticancer drug-DNA complex: Daunomycin plus d(CPGPTPAPCPG). *Proceedings of the National Academy of Sciences of the United States of America-Biological Sciences*, **77**(12): 7204–7208.
DOI: 10.1073/pnas.77.12.7204

R Core Team.
2014. R: A Language and Environment for Statistical Computing.

Raha, S. and B. H. Robinson.
2001. Mitochondria, oxygen free radicals, and apoptosis. *American Journal of Medical Genetics*, **106**(1): 62–70.

Rinn, J. L. and H. Y. Chang.
2012. Genome Regulation by Long Noncoding RNAs. *Annual Review of Biochemistry*, **81**: 145–166.
DOI: 10.1146/annurev-biochem-051410-092902

Romero-Calvo, I., B. Ocon, P. Martinez-Moya, M. Dolores Suarez, A. Zarzuelo, O. Martinez-Augustin, and F. Sanchez de Medina.
2010. Reversible Ponceau staining as a loading control alternative to actin in Western blots. *Analytical Biochemistry*, **401**(2): 318–320.
DOI: 10.1016/j.ab.2010.02.036

Ruas, J. L., J. P. White, R. R. Rao, S. Kleiner, K. T. Brannan, B. C. Harrison, N. P. Greene, J. Wu, J. L. Estall, B. A. Irving, I. R. Lanza, K. A. Rasbach, M. Okutsu, K. S. Nair, Z. Yan, L. A. Leinwand, and B. M. Spiegelman.
2012. A PGC-1α isoform induced by resistance training regulates skeletal muscle hypertrophy. *Cell*, **151**(6): 1319–1331.
DOI: 10.1016/j.cell.2012.10.050

Russo, S., W. Filippelli, F. Ferraraccio, L. Berrino, V. Guarino, and F. Rossi.
1994. Effects of *S*-adenosylmethionine (SAMe) on doxorubicin-induced cardiotoxicity in the rat. *Journal of Medicine*, **25**(1-2): 65–89.

Sadik, N. A. H., M. F. Ismail, and A. A. Shaheen.
2008. Effect of probucol and desferroxamine against adriamycin toxicity in cardiac and renal tissues of rats. *Indian Journal of Biochemistry & Biophysics*, **45**(1): 44–50.

Safdar, A., J. P. Little, A. J. Stokl, B. P. Hettinga, M. Akhtar, and M. A. Tarnopolsky.
2011. Exercise increases mitochondrial PGC-1α content and promotes nuclear-mitochondrial cross-talk to coordinate mitochondrial biogenesis. *Journal of Biological Chemistry*, **286**(12): 10605–10617.
DOI: 10.1074/jbc.M110.211466

Santos, D. L., A. J. M. Moreno, R. L. Leino, M. K. Froberg, and K. B. Wallace.
2002. Carvedilol protects against doxorubicin-induced mitochondrial cardiomyopathy. *Toxicology and Applied Pharmacology*, **185**(3): 218–227.
DOI: 10.1006/taap.2002.9532

Scarpulla, R. C.
2006. Nuclear control of respiratory gene expression in mammalian cells. *Journal of Cellular Biochemistry*, **97**(4): 673–683.
DOI: 10.1002/jcb.20743

Scarpulla, R. C.
2011. Metabolic control of mitochondrial biogenesis through the PGC-1 family regulatory network. *Biochimica Et Biophysica Acta-Molecular Cell Research*, **1813**(7): 1269–1278.
DOI: 10.1016/j.bbamcr.2010.09.019

Schindelin, J., I. Arganda-Carreras, E. Frise, V. Kaynig, M. Longair, T. Pietzsch, S. Preibisch, C. Rueden, S. Saalfeld, B. Schmid, J.-Y. Tinevez, D. J. White, V. Hartenstein, K. Eliceiri, P. Tomancak, and A. Cardona.
2012. Fiji: an open-source platform for biological-image analysis. *Nature Methods*, vol. 97: 676–682.
DOI: 10.1038/nmeth.2019

Schlame, M., D. Rua, and M. L. Greenberg.
2000. The biosynthesis and functional role of cardiolipin. *Progress in Lipid Research*, **39**(3): 257–288.
DOI: 10.1016/s0163-7827(00)00005-9

Schlame, M. and M. Ren.
2006. Barth syndrome, a human disorder of cardiolipin metabolism. *Febs Letters*, **580**(23): 5450–5455.
DOI: 10.1016/j.febslet.2006.07.022

Schulz, H.
2002. "Oxidation of fatty acids in eukaryotes". *Biochemistry of Lipids, Lipoproteins and Membranes*. Ed. by D. Vance and J. Vance. Elsevier.
DOI: 10.1016/S0167-7306(02)36007-1

Selhub, J. and J. W. Miller.
1992. The pathogenesis of homocysteinemia: interruption of the coordinate regulation by *S*-adenosylmethionine of the remethylation and transsulfuration of homocysteine. *American Journal of Clinical Nutrition*, **55**(1): 131–138.

Serrano, J., C. M. Palmeira, D. W. Kuehl, and K. B. Wallace.
1999. Cardioselective and cumulative oxidation of mitochondrial DNA following subchronic doxorubicin administration. *Biochimica et Biophysica Acta-Bioenergetics*, **1411**(1): 201–205.
DOI: 10.1016/s0005-2728(99)00011-0

Shock, L. S., P. V. Thakkar, E. J. Peterson, R. G. Moran, and S. M. Taylor.
2011. DNA methyltransferase 1, cytosine methylation, and cytosine hydroxymethylation in mammalian mitochondria. *Proceedings of the National Academy of Sciences of the United States of America*, **108**(9): 3630–3635.
DOI: 10.1073/pnas.1012311108

Simunek, T., M. Sterba, O. Popelova, M. Adamcova, R. Hrdina, and V. Gersl.
2009. Anthracycline-induced cardiotoxicity: Overview of studies examining the roles of oxidative stress and free cellular iron. *Pharmacological Reports*, **61**(1): 154–171.
DOI: 10.1016/S1734-1140(09)70018-0

Smiraglia, D. J., M. Kulawiec, G. L. Bistulfi, S. G. Gupta, and K. K. Singh.
2008. A novel role for mitochondria in regulating epigenetic modification in the nucleus. *Cancer Biology & Therapy*, **7**(8): 1182–1190.

Solem, L. E., T. R. Henry, and K. B. Wallace.
1994. Disruption of Mitochondrial Calcium Homeostasis Following Chronic Doxorubicin Administration. *Toxicology and Applied Pharmacology*, **129**(2): 214–222.
DOI: 10.1006/taap.1994.1246

Steinherz, L. J., P. G. Steinherz, C. T. C. Tan, G. Heller, and M. L. Murphy.
1991. Cardiac Toxicity 4 to 20 Years After Completing Anthracycline Therapy. *Journal of the American Medical Association*, **266**(12): 1672–1677.
DOI: 10.1001/jama.266.12.1672

Sterba, M., O. Popelova, A. Vavrova, E. Jirkovsky, P. Kovarikova, V. Gersl, and T. Simunek.
2013. Oxidative Stress, Redox Signaling, and Metal Chelation in Anthracycline Cardiotoxicity and Pharmacological Cardioprotection. *Antioxidants & Redox Signaling*, **18**(8): 899–929.
DOI: 10.1089/ars.2012.4795

Suliman, H. B., M. S. Carraway, A. S. Ali, C. M. Reynolds, K. E. Welty-Wolf, and C. A. Piantadosi.
2007. The CO/HO system reverses inhibition of mitochondrial biogenesis and prevents murine doxorubicin cardiomyopathy. *Journal of Clinical Investigation*, **117**(12): 3730–3741.
DOI: 10.1172/jci32967

Taanman, J. W.
1999. The mitochondrial genome: structure, transcription, translation and replication. *Biochimica Et Biophysica Acta-Bioenergetics*, **1410**(2): 103–123.
DOI: 10.1016/s0005-2728(98)00161-3

Tokarska-Schlattner, M., M. Zaugg, R. da Silva, E. Lucchinetti, M. C. Schaub, T. Wallimann, and U. Schlattner.
2005. Acute toxicity of doxorubicin on isolated perfused heart: response of kinases regulating energy supply. *American Journal of Physiology-Heart and Circulatory Physiology*, **289**(1): H37–H47.
DOI: 10.1152/ajpheart.01057.2004

Vasquez-Vivar, J., P. Martasek, N. Hogg, B. S. S. Masters, K. A. Pritchard, and B. Kalyanaraman.
1997. Endothelial nitric oxide synthase-dependent superoxide generation from adriamycin. *Biochemistry*, **36**(38): 11293–11297.
DOI: 10.1021/bi971475e

Ventura-Clapier, R., A. Garnier, and V. Veksler.
2004. Energy metabolism in heart failure. *Journal of Physiology-London*, **555**(1): 1–13.
DOI: 10.1113/jphysiol.2003.055095

Ventura-Clapier, R., A. Garnier, and V. Veksler.
2008. Transcriptional control of mitochondrial biogenesis: the central role of PGC-1α. *Cardiovascular Research*, **79**(2): 208–217.
DOI: 10.1093/cvr/cvn098

Waddington, C.
1957. *The Strategy of the Genes: A Discussion of Some Aspects of Theoretical Biology*. Allen & Unwin.

Wallace, D. C. and W. Fan.
2010. Energetics, epigenetics, mitochondrial genetics. *Mitochondrion*, **10**(1): 12–31.
DOI: 10.1016/j.mito.2009.09.006

Wallace, K. B.
2003. Doxorubicin-induced cardiac mitochondrionopathy. *Pharmacology & Toxicology*, **93**(3): 105–115.
DOI: 10.1034/j.1600-0773.2003.930301.x

Wang, S., P. Song, and M.-H. Zou.
2012. Inhibition of AMPKα by doxorubicin accentuates genotoxic stress and cell death in mouse embryonic fibroblasts and cardiomyocytes: role of p53 and SIRT1. *Journal of Biological Chemistry*, **287**(11): 8001–8012.
DOI: 10.1074/jbc.M111.315812

Wellen, K. E., G. Hatzivassiliou, U. M. Sachdeva, T. V. Bui, J. R. Cross, and C. B. Thompson.
2009. ATP-Citrate Lyase Links Cellular Metabolism to Histone Acetylation. *Science*, **324**(5930): 1076–1080.
DOI: 10.1126/science.1164097

Wilcox, R. R.
2012. *Introduction to Robust Estimation and Hypothesis Testing*. Academic Press.

Wilstermann, A. M. and N. Osheroof.
2003. Stabilization of eukaryotic topoisomerase II-DNA cleavage complexes. *Current Topics in Medicinal Chemistry*, **3**(3): 321–338.
DOI: 10.2174/1568026033452519

Wright, D. C., D.-H. Han, P. M. Garcia-Roves, P. C. Geiger, T. E. Jones, and J. O. Holloszy.
2007. Exercise-induced mitochondrial biogenesis begins before the increase in muscle PGC-1α expression. *Journal of Biological Chemistry*, **202**(1): 194–199.
DOI: 10.1074/jbc.M606116200

Xiong, Y., X. Liu, C.-P. Lee, B. H. Chua, and Y.-S. Ho.
2006. Attenuation of doxorubicin-induced contractile and mitochondrial dysfunction in mouse heart by cellular glutathione peroxidase. *Free Radical Biology and Medicine*, **41**(1): 46–55.
DOI: 10.1016/j.freeradbiomed.2006.02.024

Yang, F., S. S. Teves, C. J. Kemp, and S. Henikoff.
2014. Doxorubicin, DNA torsion, and chromatin dynamics. *Biochimica et Biophysica Acta-*

Reviews on Cancer, **1845**(1): 84–89.
DOI: 10.1016/j.bbcan.2013.12.002

Yen, H. C., T. D. Oberley, C. G. Gairola, L. I. Szweda, and D. K. St Clair.
1999. Manganese superoxide dismutase protects mitochondrial complex I against adriamycin-induced cardiomyopathy in transgenic mice. *Archives of Biochemistry and Biophysics*, **362**(1): 59–66.
DOI: 10.1006/abbi.1998.1011

Yokochi, T. and K. D. Robertson.
2004. Doxorubicin inhibits DNMT1, resulting in conditional apoptosis. *Molecular Pharmacology*, **66**(6): 1415–1420.
DOI: 10.1124/mol.104.002634

Zhang, C. L., T. A. McKinsey, J. R. Lu, and E. N. Olson.
2001. Association of COOH-terminal-binding protein (CtBP) and MEF2-interacting transcription repressor (MITR) contributes to transcriptional repression of the MEF2 transcription factor. *Journal of Biological Chemistry*, **276**(1): 35–39.

Zhang, Y., S. Kwon, T. Yamaguchi, F. Cubizolles, S. Rousseaux, M. Kneissel, C. Cao, N. Li, H.-L. Cheng, K. Chua, D. Lombard, A. Mizeracki, G. Matthias, F. W. Alt, S. Khochbin, and P. Matthias.
2008. Mice lacking histone deacetylase 6 have hyperacetylated tubulin but are viable and develop normally. *Molecular and Cellular Biology*, **28**(5): 1688–1701.
DOI: 10.1128/mcb.01154-06

Zhou, S. Y., A. Starkov, M. K. Froberg, R. L. Leino, and K. B. Wallace.
2001a. Cumulative and irreversible cardiac mitochondrial dysfunction induced by doxorubicin. *Cancer Research*, **61**(2): 771–777.

Zhou, S. Y., C. M. Palmeira, and K. B. Wallace.
2001b. Doxorubicin-induced persistent oxidative stress to cardiac myocytes. *Toxicology Letters*, **121**(3): 151–157.
DOI: 10.1016/s0378-4274(01)00329-0